~~Speeding up and boosting tsunami warning in Chile~~ Speeding up Tsunami Forecasting to boost Tsunami Warning in Chile

Mauricio Fuentes[1], Sebastian Arriola[2], Sebastian Riquelme[2], and Bertrand Delouis[3]

[1]Department of Geophysics, Faculty of Physical and Mathematical Sciences, University of Chile
[2]National Seismological Center, Faculty of Physical and Mathematical Sciences, University of Chile
[3]Géoazur, Université de Nice Sophia Antipolis, Observatoire de la Côte d'Azur

Correspondence: Mauricio Fuentes (mauricio@dgf.uchile.cl)

Abstract. ~~Chile host a great tsunamigenic potential along its coast, even with the large earthquakes occurred during the last decade, there is still a large amount of seismic energy to release. This permanent feature and the fact that the distance between the trench and the coast is just 100 km creates a difficult environment to do real time tsunami forecast. In Chile tsunami warnings are based on reports of the seismic events (hypocenter and magnitude) and a database of precomputed tsunami scenarios. However, because yet there is no answer to image the finite fault model within first minutes (before the first tsunami wave arrival), the precomputed scenarios consider uniform slip distributions. Here, we propose a scheme of processes to fill the gaps in-between blind zones due to waiting of demanding computational stages. The linear shallow water equations are solved to obtain a rapid estimation of the runup distribution in the near field. Our results show that this linear method captures most of the complexity of the run-up heights in terms of shape and amplitude when compared with a fully non-linear tsunami code. Also, the run-up distribution is obtained in quasi real-time as soon as the seismic finite fault model is produced.~~ Despite the occurrence of several large earthquakes during the last decade, Chile continues to have a great tsunamigenic potential. This arises as a consequence of the large amount of strain accumulated along a subduction zone that runs parallel to its long coast, and a distance from the trench to the coast of no more than 100 km. These conditions make it difficult to implement real-time tsunami forecasting. Chile issues local tsunami warnings based on preliminary estimations of the hypocenter location and magnitude of the seismic sources, combined with a database of pre-computed tsunami scenarios. Finite fault modeling, however, does not provide an estimation of the slip distribution before the first tsunami wave arrival, so all pre-computed tsunami scenarios assume a uniform slip distribution. We implemented a processing scheme that minimizes this time gap by assuming an elliptical slip distribution, thereby not having to wait for the more time consuming finite fault model computations.We then solve the linear shallow water equations to obtain a rapid estimation of the runup distribution in the near field. Our results show that, at a certain water depth, our linear method captures most of the complexity of the runup heights in terms of shape and amplitude when compared with a fully non-linear tsunami model. In addition, we can estimate the runup distribution in quasi-real-time as soon as the results of seismic finite fault modeling become available.

1 Introduction

~~For decades, coastal-exposed countries have been working on tsunami warning systems (Doi, 2003; Wächter et al., 2012). Due to the tsunami source process, most of them are attributed to large subduction earthquake or to landslides, then real-time forecast is out of reach. Regular earthquakes follow a scaling law in terms of its released energy (seismic moment) and its duration (Ide et al, 2007). For instance, a regular M_w 8.5 can last for $\approx$ 2 minutes, whereas tsunami generation is considered quasi-instantaneous after the source time. This implies that a robust tsunami warning system must be related to different monitoring systems of potential triggers (earthquakes, volcanoes, among others). In the case of tsunamis generated by subduction earthquakes, to detect and to characterize the seismic source is crucial. Nowadays, the W-phase method is the preferred for accounting large earthquakes in Chile (Riquelme et al, 2016, 2018). A first moment tensor solution can be obtained in 5 minutes. However, it is well-known that tsunami heights are highly sensitive to the spatial slip distribution of the seismic source (Geist, 2002; Ruiz et al., 2015). Even having a finite fault model, the simulation of the tsunami propagation can take several hours depending on the desired level of resolution. This is the reason why many of the current warning systems are based on precomputed scenarios. Chile and Japan use this methodology for that purpose (https://www.jma.go.jp/jma/en/News/lists/tsunamisystem2006mar.pdf). However, this methodology ignores the complexity of the seismic source resolving for uniform slip models only. In this work we propose a methodology specific for near-field tsunamis triggered by earthquakes that complements information to the operating monitoring systems and helps to make decisions during and after the emergency alert.~~ For decades, countries exposed to coastal inundation have done a lot of work to develop their tsunami warning systems (Doi, 2003; Wächter et al., 2012). Most tsunamis are generated by large subduction earthquakes and landslides, which owing to the characteristics of the tsunami source process, places a real-time tsunami forecast out of reach. Regular earthquakes follow a scaling law that links their energy release (seismic moment) to their duration (Ide et al, 2007). For instance, a regular 8.5 Mw earthquake can last for about 2 minutes, whereas we can consider tsunami generation nearly instantaneous after the source origin time. This implies that a robust tsunami warning system must integrate several systems that monitor different potential triggers such as earthquakes and volcanoes, among others. In the case of tsunamis generated by subduction earthquakes is essential to detect and characterize the seismic source. At present, the W-phase moment tensor is the preferred method for characterizing large earthquakes in Chile (Riquelme et al, 2016, 2018), as it allows to obtain a moment tensor solution within 5 minutes. It is well-known, however, that tsunami heights are very sensitive to the spatial slip distribution of the seismic source (Geist, 2002; Ruiz et al., 2015). Even after having a finite fault model, the simulation of the tsunami propagation can take several hours depending on the desired level of resolution. This is the reason why the tsunami forecasts of many of the current warning systems are based on pre-computed scenarios (Reymond et al., 2012; Gusman et al., 2014; Mulia et al., 2018). Chile and Japan use this methodology for that purpose (https://www.jma.go.jp/jma/en/News/lists/tsunamisystem2006mar.pdf). This methodology, however, ignores the complexity of the seismic source and solves only for uniform slip models. We propose a methodology applicable to near-field tsunamis triggered by earthquakes that complements the monitoring systems in operation, and helps make better decisions during and after an emergency alert.

2 Methodology

~~This problem is separated in three parts. The determination of a seismic source model, the generation of an initial condition and the corresponding tsunami simulation. We define a computation domain around the earthquake source and the coastal areas in the near field. The bathymetric data used is the SRTM15 with 15 arcsec of resolution, based on the STM30 (Becker et al., 2009). The idea here is to trade off accuracy for rapidness. In a near field earthquake tsunami context we care about the maximum inundation place, the extension of the inundation until decreases to 0.5 to 1 m, and the average run-up. This model is not trying to be as accurate as possible and to determine a detailed inundation map but what intends to do is to give an idea of the main area that is going to be affected using the W-phase CMT, which is currently one of the fastest methodology to characterize large earthquake parameters in real time (Kanamori and Rivera, 2008).~~ We can separate this problem into three main parts: 1) the estimation of a seismic source model, 2) the generation of initial conditions, and 3) the corresponding tsunami simulation. We define a computation domain around the earthquake source and the coastal areas in the near field. We use the SRTM15 bathymetric data with 15 arcsec of resolution, based on the STM30 (Becker et al., 2009).

The core idea consists in trading off some accuracy to gain speed. Within the context of tectonic tsunamis generated in the near field we want to know the places with the maximum inundation, the extension of the inundation until it decreases to 0.5 to 1 m, and the average runup. Our model does not aim at computing a detailed inundation map with the best possible accuracy, but rather to provide a fast estimate of the main area prone to inundation relying on the W-phase CMT, currently considered one of the fastest and more accurate methods to characterize the source of large earthquake (Kanamori and Rivera, 2008).

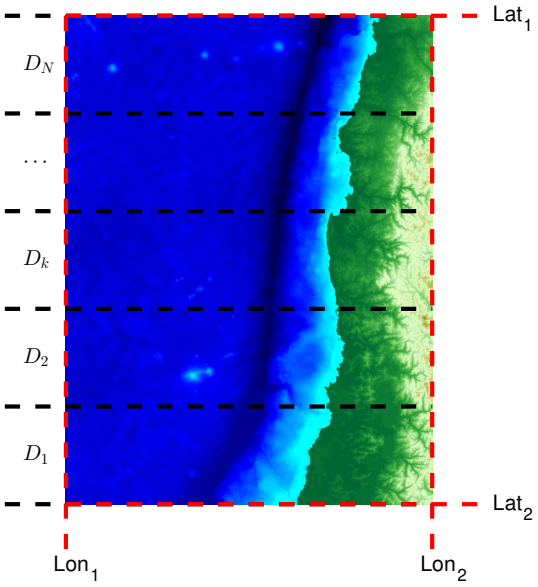

Figure 1. ~~Sketch of the partition of the computation domain for parallel running.~~ Schematic showing the discretization of the calculation domain for parallel computation.

2.1 ~~The~~ ~~s~~ S lip ~~d~~ D istribution ~~m~~ M odel

~~Once an earthquake is firstly described by the W-phase solution, we use an elliptical slip distribution (Dmowska and Rice, 1986) over a region determined with the scaling laws obtained by Blaser et al. (2010). This serves as a first estimation while seismic waves are still traveling, and subsequent finite fault solutions are computed. Thus, we can model the near field tsunami for every finite fault model update.~~ Once a W-phase solution provides a characterization of an earthquake we use an elliptical slip distribution (Dmowska and Rice, 1986) over a region determined with the scaling laws obtained by Blaser et al. (2010). This serves as a preliminary estimation while seismic waves are still traveling, and later finite fault solutions are computed. This in turn allows to model the near field tsunami for every finite fault model update. The elliptic model is discretized with n_y subfaults along-dip and $n_x = \lceil \frac{L}{W} n_y \rceil$, where L and W are the length and width of the fault plane obtained with the scaling law. With $n_y = 16$, all the studied cases have enough resolution on the source area.

2.2 ~~The~~ ~~t~~ T sunami ~~i~~ I nitial ~~c~~ C onditions

~~Despite there are evidences of influence in the tsunami generation process with the source time components, for quickness purposes, we model static seafloor deformation induced by a non-uniform slip distribution including the horizontal components, as suggested in Tanioka and Satake (1996). This is obtained with that Okada's equations (Okada, 1985).~~ Despite evidence of influence of the source time components in the tsunami generation process, for speed purposes we model a static seafloor deformation induced by a non-uniform slip distribution that includes the horizontal components, as suggested in Tanioka and Satake (1996). This is obtained by applying the Okada equations (Okada, 1985).

2.3 ~~The~~ ~~t~~ T sunami ~~m~~ M odeling

~~The last part of this methodology is to obtain the tsunami heights along the coast. Usually, tsunami modeling involves complex codes to solve the fully coupled non-linear shallow water equations. Depending on the domain size and resolution, a full tsunami run can take several hours, which make real-time forecast impossible. To overcome this limitation, we solve the linear shallow water equations with a forward finite difference scheme. The propagation inside the domain is governed by the second order PDE with initial conditions:~~ The last part of this methodology is the estimation of the tsunami heights along the coast. Usually, tsunami modeling involves complex codes to solve the fully coupled non-linear shallow water equations. Depending on the domain size and resolution, a full tsunami simulation run can take several hours, which makes real-time forecast nearly impossible. To overcome this limitation, we solve the linear shallow water equations with a forward finite difference scheme. The propagation inside the domain is governed by the second order PDE with initial conditions:

$$\begin{aligned} \eta_{tt} - g\nabla\left(h\nabla\eta\right) &= 0 \\ \eta(x,y,0) &= \eta_0(x,y) \\ \eta_t(x,y,0) &= 0 \end{aligned} \tag{1}$$

where $\eta(x,y,t)$ ~~is~~ denotes the water surface, g ~~is~~ the ~~gravity~~ acceleration of gravity, $h(x,y)$ ~~is~~ the bathymetry and $\eta_0(x,y)$ ~~is~~ the initial condition. In the open boundaries, we set a radiation condition (Reid and Bodine, 1968), whereas in the solid boundaries (coasts) we impose full reflection in a vertical wall placed at an isobath of 100 m, before ~~to reach~~ reaching the non-linear zone. Here, a Neumann boundary condition is applied: $\frac{\partial \eta}{\partial \hat{\boldsymbol{n}}}$ where $\hat{\boldsymbol{n}}$ denotes the exterior unit normal vector. The linear method (~~hereafter,~~ LM) allows to obtain a quicker estimation than a full tsunami code since second-order terms are ~~neglected but keeping~~ disregarded while still accounting for the same main features. ~~Also~~ In addition , this approach does not require ~~to compute~~ computing the velocity field, ~~making the~~ an added benefit that makes the computation programs even faster. Each simulation is compared ~~with a fully~~ to its corresponding full non- linear ~~water~~ shallow water equation propagation. We ~~select~~ use the JAGURS code (Baba et al., 2014) ~~which runs~~ written in Fortran90 ~~in a~~ using parallel arrays via ~~with~~ OpenMP and OpenMP + MPI. This code is based ~~in~~ on the classical finite difference method of Satake (2002). For each scenario, ~~the tsunami is propagated during two hours of tsunami time,~~ we run the simulation for the equivalent of two hours of tsunami travel time to obtain the main features of the runup distributions, despite the fact that later amplification of edge waves and resonances effects can occur. The approximated runup is obtained as the maximum from the vertical wall reflexion boundary condition. This is usually on the same order with the actual runup in a sloping beach model (Synolakis, 1987).

3 ~~Tests and results~~ Implementation and Benchmarking

~~For evaluating the performance of this simple approach, we have modeled nearly all of the great tsunamis in the last two decades. Most of them were already tested with an analytical approach in (Riquelme et al, 2015). The details of the propagation and runup distribution of the 12 events tested are exhibited in the supporting information. For these examples we used the finite fault models obtained from USGS (Hayes, 2017), because they have proven to be operational and robust for real time operations in a global context monitoring. All the computations were performed in a Dell Precision 7920, with two Intel Xeon Gold 6136 processor, 12 physical core each, for a total of 24 physical core, 2 threads each. For each time iteration, the domain is divided in 48 subdomains that are computed in different threads, for a parallel array (Fig. 1). To compute the tsunami initial condition, the Okada's equations were implemented in C language using threading, as well as the finite difference scheme for the LM. The C code uses pthread library. With this tool, a data struct containing a pthread_t was defined, and then a routine that send every grid's subdomain to each different core's thread for computation. This method is such reliable as any other linear scheme method, because it solves the same equations. The only significant difference is the threads distribution for time optimization. When a thread finishes, it computes for a certain time step and it joins with the others in order to avoid miscomputations. For instance, with the used machine, in a regular grid of 4 million points with a FFM of 300 subfaults, the vertical and horizontal seafloor displacements can be calculated almost instantly (less than 5 seconds) and two hours of tsunami propagation for 2011 Tohoku, Japan earthquake can be solved in 60 seconds.~~ To evaluate the performance of our approach, we modeled nearly all the great tsunamis of the last two decades. Most of them were already tested with an analytical approach in (Riquelme et al, 2015). The details of the propagation and runup distribution of the 12 events tested are presented in the supporting information. For these examples we used the finite fault models provided by the USGS (Hayes, 2017), as they

have proven to be operationally robust for real time operations in the context of global monitoring. All the computations were performed in a Dell Precision 7920, with two Intel Xeon Gold 6136 processors, each with 12 physical cores, for a total of 24 physical cores, and 2 threads each. For each time iteration, the domain is divided into 48 subdomains that are computed in different threads, for a parallel array (Fig.1). To compute the tsunami initial condition, the Okada equations were implemented in the C programming language using threading, together with the finite difference scheme for the LM. The C code uses the pthread library to define a C data structure containing a pthread, and then calls a function that sends each grid subdomain to threads running in different cores for computation. This method is as reliable as any other linear scheme method, as it solves the same equations. The only significant difference is in the threads distribution for time optimization. When a thread finishes, it computes for a certain time step and it joins with the others in order to avoid miscomputations. For instance, on the system used to run our computations for a regular grid of 4 million points with an FFM of 300 subfaults, the vertical and horizontal seafloor displacements can be calculated almost instantly (less than 5 seconds), and two hours of tsunami wave propagation for the 2011 Tohoku, Japan earthquake can be solved in 60 seconds.

4 ~~Examples~~ Discussion of Computational Results

~~All the earthquakes presented here, have produced tsunamis. The range of magnitude varies from 7.7 to 9.1. They occurred in different subduction zones around the world. The largest ones are Tohoku in Japan and Maule in Chile. All of them show a thrust mechanism except for the Samoa event in 2009 which is a normal event. There are a few tsunami earthquakes in this section such as the 1992 Mw 7.7 Nicaragua Earthquake, The 2006 Mw 7.6 Java earthquake. The extension of the earthquakes varies from $L = 150$ km to $L = 500$ km, the range of peak displacement at the source varies from 3 m to 40 m. Therefore, we have tested as many earthquakes and as many source features as possible for this study.~~ All the earthquakes presented here, have produced tsunamis. The range of magnitude varies from 7.7 to 9.1. They occurred in different subduction zones around the world. The largest ones are Tohoku in Japan and Maule in Chile. All of them show a thrust mechanism except for the Samoa event in 2009 which is a normal event. There are a few tsunami earthquakes in this section such as the 1992 Mw 7.7 Nicaragua Earthquake, The 2006 Mw 7.6 Java Earthquake. The extension of the earthquakes varies from $L = 150$ km to $L = 500$ km, the range of peak displacement at the source varies from 3 m to 40 m. Therefore, we have tested as many earthquakes and as many source features as possible for this study.

1. The 1992 Mw 7.7 Nicaragua Tsunami Earthquake
2. The 2001 Mw 8.4 Southern Perú Earthquake
3. The 2003 Mw 8.3 Hokkaido Earthquake
4. The 2006 Mw 7.6 Java Earthquake
5. The 2007 Mw 8.1 Solomon Islands Earthquake
6. The 2007 Mw 8.0 Pisco Earthquake

7. The 2009 Mw 8.1 Samoa Islands Region Earthquake
8. The 2010 Mw 8.8 Maule Earthquake
9. The 2011 Mw 9.0 Tohoku Earthquake
10. The 2012 Mw 7.8 British Columbia Earthquake
11. The 2014 Mw 8.2 Iquique Earthquake
12. The 2015 Mw 8.3 Illapel Earthquake

~~For each event we apply the methodology described before. By using the W-phase centroid moment tensor, a scaling law, and a elliptic slip distribution, the first source is defined. Then, the linear and non-linear tsunami simulations are performed. The resulting runup distributions are decomposed along latitude and longitude, in order to compare both models. The same procedure is repeated but instead considering a FFM solution. Table 1 shows the correlation of the runup distributions between the code JAGURS and the presented here (the linear method). Table 2 summaries the CPU times for each stage of the process for each simulation. There is a high degree of agreement within a short time. Detailed figures of the 24 simulations are provided in the supplementary material, where maximum amplitudes, runup distribution and field measurements are displayed.~~ For each event we apply the methodology previously described, and use the W-phase centroid moment tensor, a scaling law, and an elliptic slip distribution to define the first source. Then, the linear and non-linear tsunami simulations are performed. The resulting runup distributions are decomposed along latitude and longitude in order to compare both models. The same procedure is repeated, this time considering an FFM solution instead. Table 1 shows the correlation between the runup distributions obtained with the JAGURS code (non-linear method) and the method presented in this paper (linear method). Table 2 summarizes the CPU times in seconds for different stages of the process for each simulation. There is a high degree of agreement within a short time. Detailed figures showing the results for the 24 simulations are provided in the supplementary material, where maximum amplitudes, runup distribution, and field measurements are listed. For comparison purposes, the event of 2014 Chile, the DART station 32401 registered 0.25 m of amplitude (An et al., 2014), where the linear method predicts 0.39 m for the elliptic source and 0.12 m for the FFM, whereas JAGURS gives 0.55 m for the elliptic source and 0.15 m for the FFM.

5 Application to compliment tsunami alert. Case study: The 2015 Illapel Earthquake

~~The September 16th a 8.3 Mw earthquake took place in the Coquimbo region in Chile (Melgar et al., 2016; Fuentes et al., 2017). The features of the event were optimals for a tsunami generation. The national agencies deployed the protocols for evacuating the whole chilean coast, even in distant insular territories (SNAM, bulletin #1, Sept. 16th, 23:02 UTC). The decision has to be made the very minutes after the origin time. In general, an accurate prediction of the tsunami runup heights requires a precise image of the seismic source, which nowadays is not available within 5 minutes and worst for real-time by adding the tsunami calculation times. Nevertheless, we can stay close of and quasi real time approach and trigger a first estimation based on the~~

Table 1. ~~Correlation of the runup distribution between the linear solution and the JAGURS code.~~ Correlation of the runup distribution obtained from our linear model solution and the JAGURS code. Correlation is computed with the standard Pearson coefficient. Details can be found in the supplemental material.

Event	FFM lon	FFM lat	Elliptic lon	Elliptic lat
1992 Nicaragua	0.8323	0.8088	0.8841	0.8587
2001 Perú	0.8334	0.8575	0.6697	0.7549
2003 Japan	0.7753	0.7838	0.9139	0.9129
2006 Indonesia	0.7483	0.8531	0.8134	0.9030
2007 Solomon Isl.	0.6422	0.7575	0.8412	0.8626
2007 Perú	0.8380	0.8085	0.8872	0.8896
2009 Samoa	0.6987	0.7353	0.7779	0.8093
2010 Chile	0.7346	0.6039	0.8682	0.7820
2011 Japan	0.8571	0.7074	0.9229	0.8311
2012 Canada	0.6829	0.6034	0.8731	0.8398
2014 Chile	0.7833	0.6473	0.9051	0.8341
2015 Chile	0.9103	0.7663	0.9603	0.8686

Table 2. ~~Results of the CPU time of each event, in seconds. t_{IC} is the time for computing the initial condition, t_{Pr} the time of processing, t_{TP} the time of the tsunami propagation and t_T is the total time.~~ Summary of the CPU time in seconds for the twelve events. t_{IC} indicates the time needed to compute the initial conditions, t_{Pr} the processing time, t_{TP} the time to compute the tsunami propagation, and t_T the total time.

Event	FFM		Elliptic		LM	JAGURS	Total time t_T			
	t_{IC}	t_{Pr}	t_{IC}	t_{Pr}	t_{TP}	t_{TP}	FFM-LM	FFM-JAGURS	Elliptic-LM	Elliptic-JAGURS
1992 Nicaragua	6	4	8	5	31	575	41	585	44	586
2001 Perú	5	3	7	3	18	360	26	368	28	370
2003 Japan	5	3	9	3	22	428	30	436	34	440
2006 Indonesia	4	3	7	2	20	358	27	365	29	367
2007 Solomon Isl.	8	5	10	5	28	658	41	671	43	673
2007 Perú	4	4	9	4	31	546	39	554	44	559
2009 Samoa	4	3	6	2	17	321	24	328	25	329
2010 Chile	7	4	9	5	32	651	43	662	46	665
2011 Japan	6	6	13	6	46	223	58	235	65	242
2012 Canada	2	1	4	1	15	153	18	156	20	158
2014 Chile	5	4	11	5	24	500	33	509	40	516
2015 Chile	4	4	8	4	27	500	35	508	39	512

~~previous elliptical source. Because this can be done in a few seconds, it can be done at the moment instead searching in a precomputed data base of scenarios that are usually restricted. For monitoring purposes, the results can be updated every time a seismic source imaging is received, for both, the near field (at 15 arcsec) and regional field (at 60 arcsec). The whole information is summarized in a coded-color map, following the official coding from the Chilean institutions (Melgar et al., 2016). Color coded maps are self-explicative, which make them easy to interpret (Figures 2 and 3). Each region can be rapidly assigned with a color which deploy an specific protocol for evacuation. All the simulations were performed with two hours of propagation, where the main energy content plays a key role on the inundation process. Figure 4 exhibits the normalized energy rate that generates the runup history along the coast, showing that majority of the global energy is concentrated within the first hour. We can also observe that the first estimation made with the elliptic fault predicts the same levels of inundation as the further finite fault model in the near field, and with minor differences in the regional field. This agrees the common sense where finite fault models act in the monitory stage and time is not as critic as in the very first minutes. For completeness purposes, travel times isochrones are computed along the pacific basin (Figure 5). This is performed by computing a dense set of rays following Sandanbata et al. (2018), which allows to include dispersive effects. Also, we have included the effect of the earth elasticity as shown in An and Liu (2016). This kind of maps can be computed instantly with the very first estimation of the moment tensor and then update.~~ On 16 September, 2017 an 8.3 Mw earthquake occurred in the Coquimbo region, Chile (Melgar et al., 2016; Fuentes et al., 2017). The characteristics of this event made it an ideal case study for tsunami generation. The national agencies implemented the established protocols for evacuating the whole Chilean coast, even the more distant insular territories (SNAM, bulletin 1, Sept. 16th, 23:02 5 UTC). Such decisions have to be made within minutes of origin time. In general, an accurate prediction of the tsunami runup heights requires a precise image of the seismic source, which at present is not available within 5 minutes for real-time after adding the tsunami simulation times. Nevertheless, we can come close to a quasi-real-time approach by triggering a first estimation assuming an elliptical slip distribution. This only takes a few seconds, and can at present be done instead of searching a pre-computed database of scenarios that are usually limited. For monitoring purposes, the results can be updated everytime a seismic source imaging is received, for both, the near field (at 15 arcsec) and regional field (at 60 arcsec). All this information is summarized in a color-coded map following the official coding used by the Chilean institutions (Melgar et al., 2016). Color coded maps are self-explanatory, which makes them easy to interpret (Figs.2 and 3). Each region can then be rapidly assigned a color linked to an specific evacuation protocol. All the simulations were performed for two hours of tsunami propagation where the main energy content plays a key role on the inundation process. Figure 4 illustrates the normalized energy rate that generates the runup history along the coast, showing that the majority of the global energy is concentrated within the first hour. We can also observe that the first estimation obtained for an elliptical fault predicts the same levels of inundation as the full finite fault model in the near field, while we can observe minor differences in the regional field. This makes sense since finite fault model results become available during the tsunami monitoring stage, when time is not as critical as in the very first minutes after origin time. It has to be noticed that is possible to increase the number of warning levels allowing to find the optimal number of states for emitting and communicating the warning bulletin. In this study we choose the UNESCO standard. For completeness, we computed the travel time isochrones across the Pacific Basin (Fig. 5). These computations use a dense set of rays following Sandanbata et al. (2018), which allows to include dispersive effects.

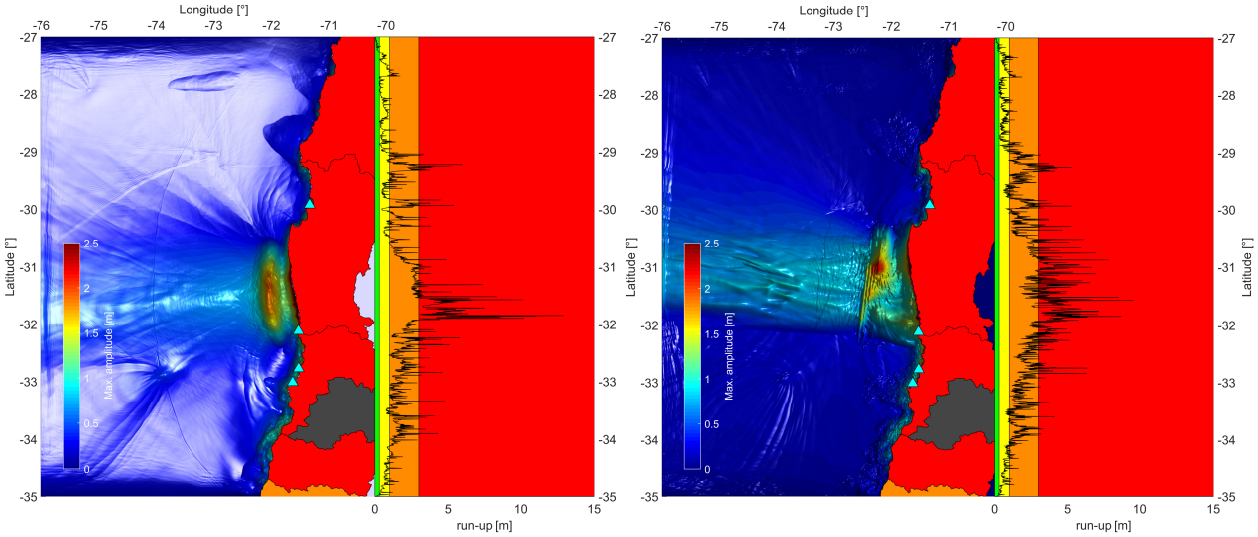

Figure 2. ~~Near Field Simulation of the 2015 Illapel Earthquake for elliptic source (left) and finite fault model (right). Red color represents the run-ups larger than 3 meters. Orange color is between 1 m and 3 m. Yellow color ranges between 0.3 m and 1 m. Green color codes run-ups smaller than 0.3 m.~~ Near field simulation of the 2015 Illapel earthquake with an elliptical source (left), and a finite fault model (right). The colors assigned to different areas indicate the expected runups in meters: a) red for runups larger than 3 m, b) orange for runups between 1 and 3 m, c) yellow for runups between 0.3 and 1 m, and d) green for runups smaller than 0.3 m.

We have also included the effect of the earth elasticity as shown in An and Liu (2016). These kind of maps can be computed instantly together with the very first estimation of the moment tensor and then updated.

6 ~~Discussion and~~ Conclusions

~~Despite linear theory has been used in other tsunami warning systems, for instance, in the PTWC (http://unesdoc.unesco.org/images/0022/002203/220368e.pdf), now it is used in combination with more complex sources and faster algorithms with an unique and simple product easy to interpret. The non-complexity of the source, does not seem to be a problem when it comes to do a fast run-up estimation regarding emergency response. Establishing levels of hazard in real time, tries to generate a more accurate extension of the area affected by the tsunami, the maximum inundation that can reach, and how many people will be exposed to this hazard along the chilean coast. This method intends to rapidly predict the run-up distribution. Using some simplifications in the tsunami equations it is possible to model rapidly the observed run-up. Obviously, this is not a high performance computing code, but even with many details outside the modeling such as complexity of the source, fine bathymetry and simplified equations, it can predict an important percentage of the run-up. The idea of extension even without the mathematical rigorosity we would like, is not inexact when we think of the idea of an emergency response system that needs to trigger actions that can save lives and reduce economic losses after the occurrence of a large earthquake.~~

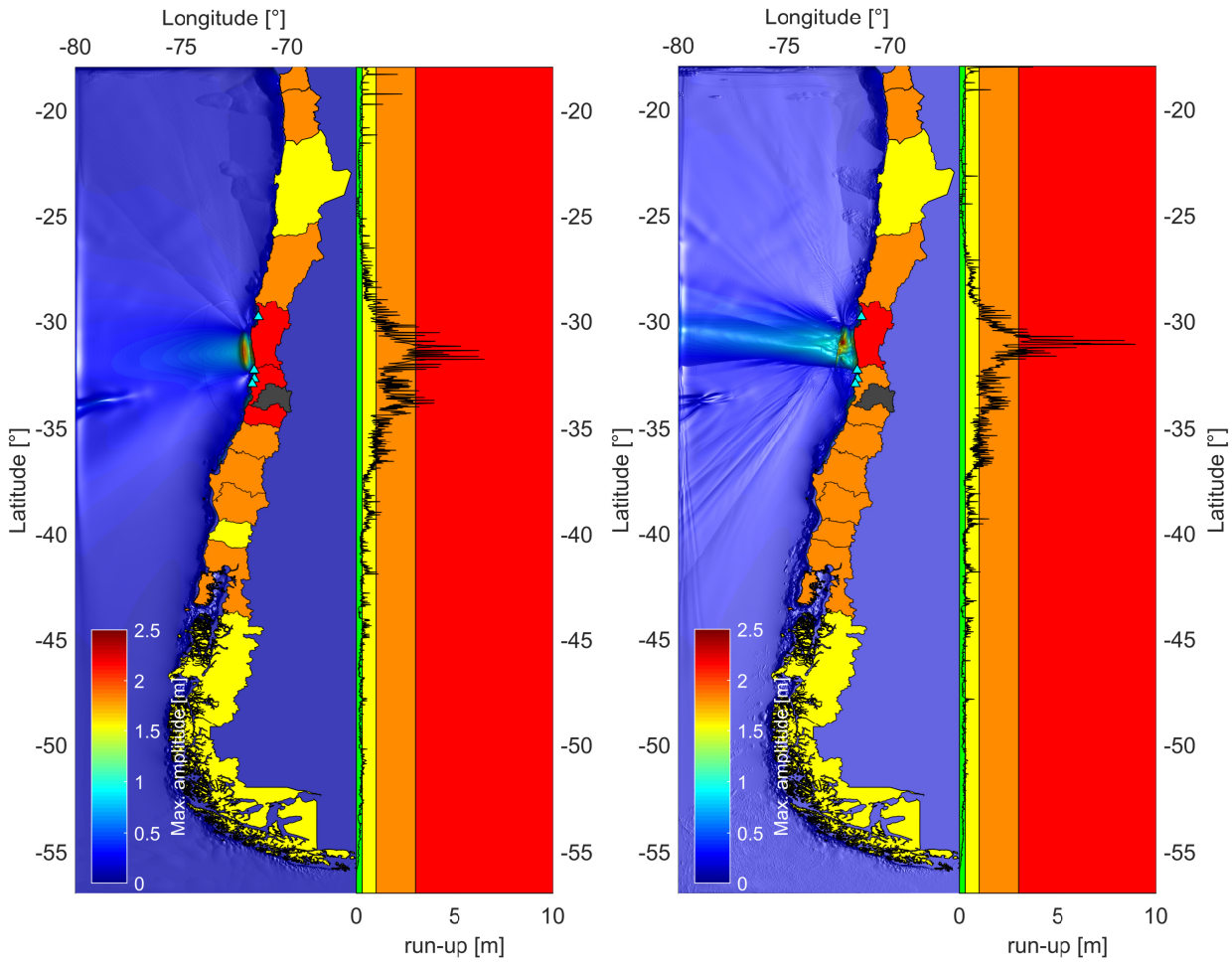

Figure 3. ~~Regional Field Simulation of the 2015 Illapel Earthquake for elliptic source (left) and finite fault model (right). Red color represents the run-ups larger than 3 m. Orange color is between 1 m and 3 m. Yellow color ranges between 0.3 m and 1 m. Green color codes run-ups smaller than 0.3 m.~~ Regional field simulation of the 2015 Illapel earthquake for an elliptical source (left), and a finite fault model (right). The colors assigned to different areas indicate the expected runups in meters: a) red for runups larger than 3 m, b) orange for runups between 1 and 3 m, c) yellow for runups between 0.3 and 1 m, and d) green for runups smaller than 0.3 m.

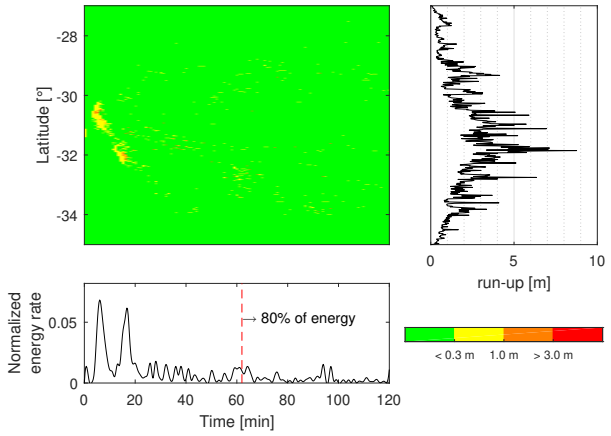

Figure 4. ~~Normalized run-up energy rate during the first two hours of tsunami simulation. Upper left panel display the run-up rate along latitude and time. Upper right panel shows the final maximum run-up and bottom left panel exhibits the normalized energy rate of the whole process as a time series.~~ Normalized runup energy rate during the first two hours of tsunami simulation. The upper left panel shows the runup rate along latitude and time, the upper right panel shows the final maximum runup, and the bottom left panel shows the normalized energy rate for the whole process as a time series.

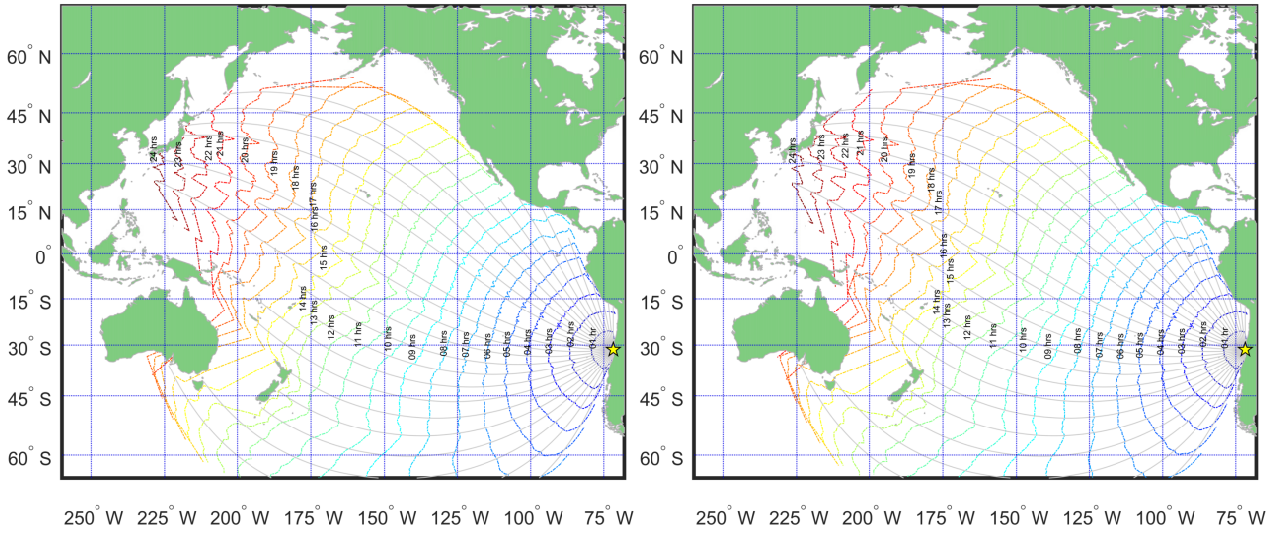

Figure 5. ~~Travel times along the pacific basin due to the 2015 Illapel Earthquake. Left panel is purely Shallow Water and right panel includes dispersion and earth elasticity for a wave frequency of 2 mHz.~~ Tsunami travel times across the Pacific basin for the 2015 Illapel earthquake.The left panel shows the travel times after the shallow water equations, while the travel times in the right panel include the effects of dispersion and the earth elasticity for a wave frequency of 2 mHz.

~~Using the methodology of Sandanbata et al. (2018) it is possible to instantaneously calculate the tsunami arrival times from sources generated in the far field. This can also be done using tsunami modeling, however this takes a longer time of calculation then this numerical methodology is accurate enough to calculate tsunami travel times from far field events. When we compare it with tsunami modeling codes, such as JAGURS, this method includes more than 80% of the predicted run-up in a 15 arcsec bathymetry at least 20 times faster. The main purpose of this study is to produce fast run-up estimations with reasonable accuracy. The idea here is to compliment the tsunami warning information while full and long calculations are being done (Figure 6). This simple method provide simple and reliable information about the tsunami threat, which allows to entities to take decisions properly.~~ In this study we propose a method that disregards the fine complexity of the seismic source while using fine bathymetric data and a set of simplified equations to model more than 80% of the runups with enough accuracy for tsunami warning purposes up to 20 times faster. Our method also aims at rapidly predicting the spatial distribution of the runups using some simplifications in the tsunami equations. Despite lacking the mathematical rigorosity that we would otherwise prefer, the method we propose is not inexact within the context of an emergency response system that needs to trigger actions that can potentially save lives and reduce economic losses after the occurrence of a large earthquake. We summarized our approach in a flow chart (Fig. 6). Taking into account the results of our study we can list the following as the most noteworthy results:

1. Although other tsunami warning centers use linear theory as part of their operations, for instance at the PTWC (http://unesdoc.unesco.org/images/0022/002203/220368e.pdf), in this study we have combined it with the use of more complex sources and faster algorithms to generate a unique and simple product easy to interpret.

2. The non-complexity of the adopted source does not seem to significantly affect the results of a fast runup estimation for emergency response purposes. By computing different levels of tsunami hazard in near-real time we estimate more accurately the extent of the area potentially affected by the tsunami, the maximum level of inundation, and how many people will be exposed to this hazard along the Chilean coast.

3. Using the methodology of Sandanbata et al. (2018) it is possible to instantaneously calculate the tsunami arrival times from sources generated in the far field with enough accuracy. This can also be done via tsunami modeling, but at the expense of longer computation times.

4. When compared to other tsunami modeling codes such as JAGURS, results obtained from our method match more than 80% of the predicted runup for 15 arcsec bathymetry while obtaining the results at least 20 times faster.

5. The simple method proposed in this study provides a fast, reliable, and intuitive characterization of the tsunami threat, which in turn allows disaster mitigation agencies to take appropriate action.

Acknowledgements. This study was enterally supported by the *Programa de Riesgo Sśmico*.

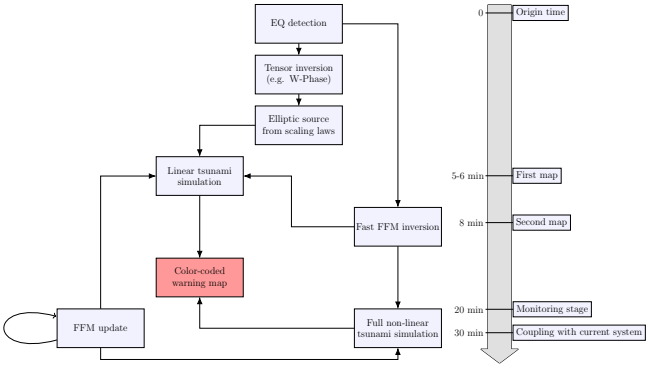

Figure 6. ~~Flow chart of the proposed methodology.~~ Flow chart of the methodology proposed in this study.

References

AN, C., SEPÚLVEDA, I., AND LIU, P. L. F. *Tsunami source and its validation of the 2014 Iquique, Chile, earthquake.* Geophysical Research Letters, 41(11), 3988-3994, 2014.

AN, C., AND LIU, P. L.: *Analytical solutions for estimating tsunami propagation speeds*, Coastal Engineering, 117, 44-56, 2016.

BABA, T., TAKAHASHI, N., KANEDA, Y., INAZAWA, Y., KIKKOJIN, M.: *Tsunami Inundation Modeling of the 2011 Tohoku Earthquake Using Three-Dimensional Building Data for Sendai, Miyagi Prefecture, Japan.*, In: Kontar Y., Santiago-Fandiño V., Takahashi T. (eds) Tsunami Events and Lessons Learned. Advances in Natural and Technological Hazards Research, 35. Springer, Dordrecht, 2014.

BECKER, J. J., SANDWELL, D. T., SMITH, W. H. F., BRAUD, J., BINDER, B., DEPNER, J., FABRE, D., FACTOR, J., INGALLS, S., KIM, S-H., LADNER, R.,MARKS, K., NELSON, S., PHARAOH, A., SHARMAN, G., TRIMMER, R., VON ROSENBURG, J., WALLACE G., AND WEATHERALL, P.: *Global bathymetry and elevation data at 30 arc seconds resolution: SRTM30_PLUS*, Marine Geodesy, 32(4), 355-371, 2009.

BLASER, L., KRÜGER, F., OHRNBERGER, M., AND SCHERBAUM, F.: *Scaling relations of earthquake source parameter estimates with special focus on subduction environment*, Bulletin of the Seismological Society of America, 100(6), 2914-2926, 2010.

DOI, K.: *Tsunami Warning System in Japan*, In: Zschau J., Küppers A. (eds) Early Warning Systems for Natural Disaster Reduction. Springer, Berlin, Heidelberg, 2003.

DMOWSKA, R., AND RICE, J. R.: *Fracture theory and its seismological applications*, Continuum Theories in Solid Earth Physics, 3, 187-255, 1986.

FUENTES, M., RIQUELME, S., HAYES, G., MEDINA, M., MELGAR, D., VARGAS, G., GONZALEZ, J., AND VILLALOBOS, A.: *A study of the 2015 Mw 8.3 Illapel earthquake and tsunami: Numerical and analytical approaches*, In The Chile-2015 (Illapel) Earthquake and Tsunami, 255-266. Birkhäuser, Cham, 2017.

GEIST, E. L.: *Complex earthquake rupture and local tsunamis*, Journal of Geophysical Research: Solid Earth, 107(B5), 2002.

GUSMAN, A.R., TANIOKA, Y., MACINNES, B.T. AND TSUSHIMA, H.: *A methodology for near-field tsunami inundation forecasting: Application to the 2011 Tohoku tsunami*, J. GEOPHYS. RES.: SOLID EARTH, 119(11), 8186-8206, 2014.

HAYES, G.: *The finite, kinematic rupture properties of great-sized earthquakes since 1990*, Earth and Planetary Science Letters 468, 94-100, 2017.

IDE, S., BEROZA, G. C., SHELLY, D. R., AND UCHIDE, T.: *A scaling law for slow earthquakes*, Nature, 447(7140), 76-79, 2007.

KANAMORI, H., AND RIVERA, L.: *Source inversion of Wphase: speeding up seismic tsunami warning*, Geophysical Journal International, 175(1), 222-238, 2008.

MELGAR, D., ALLEN, M., RIQUELME, S., GENG, J., LIANG, C., BRAVO, F., BAEZ, J.C., PARRA, H., BARRIENTOS, S., PENG, F., BOCK, Y., BEVIS, M., CACCAMISE, DANA., VIGNY, C., MORENO, M., AND SMALLEY, R.: *Local tsunami warnings: Perspectives from recent large events.*, Geophysical Research Letters, 43(3), 1109-1117, 2016.

MULIA, I. E., GUSMAN, A. R., AND SATAKE, K.: *Alternative to non-linear model for simulating tsunami inundation in real-time*. Geophysical Journal International, 214(3), 2002-2013, 2018.

OKADA, Y.: *Surface deformation due to shear and tensile faults in a half-space*, Bulletin of the seismological society of America, 75(4), 1135-1154, 1985.

REID, R. O., AND BODINE, B. R.: *Numerical model for storm surges in Galveston Bay*, Journal of the Waterways and harbors Division, 94(1), 33-58, 1968.

REYMOND, D., OKAL, E. A., HÉBERT, H., AND BOURDET, M. *Rapid forecast of tsunami wave heights from a database of pre-computed simulations, and application during the 2011 Tohoku tsunami in French Polynesia*. Geophysical Research Letters, 39(11), 2012.

RIQUELME, S., FUENTES, M., HAYES, G. P., AND CAMPOS, J.: *A rapid estimation of near-field tsunami runup*, Journal of Geophysical Research: Solid Earth, 120(9), 6487-6500, 2015.

RIQUELME, S., BRAVO, F., MELGAR, D., BENAVENTE, R., GENG, J., BARRIENTOS, S., AND CAMPOS, J.: *W phase source inversion using high-rate regional GPS data for large earthquakes*, Geophysical Research Letters, 43(7), 3178-3185, 2016.

RIQUELME, S., MEDINA M., BRAVO, F., BARRIENTOS, S., CAMPOS, J. AND CISTERNAS A.: *W-phase Real Time Implementation and Network Expansion: The Experience in Chile 2012-2017s*, Seismological Research Letters, 89(6), 2237-2248, 2018.

RUIZ, J. A., FUENTES, M., RIQUELME, S., CAMPOS, J., AND CISTERNAS, A.: *Numerical simulation of tsunami runup in northern Chile based on non-uniform k-2 slip distributions*, Natural Hazards, 79(2), 1177-1198, 2015.

SATAKE, K.: *Tsunamis*, In: Lee WHK, Kanamori H, Jennings PC, Kisslinger C (eds) International handbook of earthquake and engineering seismology, vol 81A. Academic, Amsterdam, 437-451, 2002.

SYNOLAKIS, C. E. *The runup of solitary waves*. Journal of Fluid Mechanics, 185, 523-545.

TANIOKA, Y., AND SATAKE, K.: *Tsunami generation by horizontal displacement of ocean bottom*, Geophysical Research Letters, 23(8), 861-864, 1996.

SANDANBATA, O., WATADA, S., SATAKE, K., FUKAO, Y., SUGIOKA, H., ITO, A., AND SHIOBARA, H.: *Ray Tracing for Dispersive Tsunamis and Source Amplitude Estimation Based on Green's Law: Application to the 2015 Volcanic Tsunami Earthquake Near Torishima, South of Japan*, Pure and Applied Geophysics, 175(4), 1371-1385, 2018.

WÄCHTER, J., BABEYKO, A., FLEISCHER, J., HÄNER, R., HAMMITZSCH, M., KLOTH, A., AND LENDHOLT, M.: *Development of tsunami early warning systems and future challenges*, Natural Hazards and Earth System Sciences, 12(6), 1923-1935, 2012.

Speeding up Tsunami Forecasting to boost Tsunami Warning in Chile

Mauricio Fuentes[1], Sebastian Arriola[2], Sebastian Riquelme[2], and Bertrand Delouis[3]

[1]Department of Geophysics, Faculty of Physical and Mathematical Sciences, University of Chile
[2]National Seismological Center, Faculty of Physical and Mathematical Sciences, University of Chile
[3]Géoazur, Université de Nice Sophia Antipolis, Observatoire de la Côte d'Azur

Correspondence: Mauricio Fuentes (mauricio@dgf.uchile.cl)

Abstract. Despite the occurrence of several large earthquakes during the last decade, Chile continues to have a great tsunamigenic potential. This arises as a consequence of the large amount of strain accumulated along a subduction zone that runs parallel to its long coast, and a distance from the trench to the coast of no more than 100 km. These conditions make it difficult to implement real-time tsunami forecasting. Chile issues local tsunami warnings based on preliminary estimations of the hypocenter location and magnitude of the seismic sources, combined with a database of pre-computed tsunami scenarios. Finite fault modeling, however, does not provide an estimation of the slip distribution before the first tsunami wave arrival, so all pre-computed tsunami scenarios assume a uniform slip distribution. We implemented a processing scheme that minimizes this time gap by assuming an elliptical slip distribution, thereby not having to wait for the more time consuming finite fault model computations.We then solve the linear shallow water equations to obtain a rapid estimation of the runup distribution in the near field. Our results show that, at a certain water depth, our linear method captures most of the complexity of the runup heights in terms of shape and amplitude when compared with a fully non-linear tsunami model. In addition, we can estimate the runup distribution in quasi-real-time as soon as the results of seismic finite fault modeling become available.

1 Introduction

For decades, countries exposed to coastal inundation have done a lot of work to develop their tsunami warning systems (Doi, 2003; Wächter et al., 2012). Most tsunamis are generated by large subduction earthquakes and landslides, which owing to the characteristics of the tsunami source process, places a real-time tsunami forecast out of reach. Regular earthquakes follow a scaling law that links their energy release (seismic moment) to their duration (Ide et al, 2007). For instance, a regular 8.5 Mw earthquake can last for about 2 minutes, whereas we can consider tsunami generation nearly instantaneous after the source origin time. This implies that a robust tsunami warning system must integrate several systems that monitor different potential triggers such as earthquakes and volcanoes, among others. In the case of tsunamis generated by subduction earthquakes is essential to detect and characterize the seismic source. At present, the W-phase moment tensor is the preferred method for

characterizing large earthquakes in Chile (Riquelme et al, 2016, 2018), as it allows to obtain a moment tensor solution within 5 minutes. It is well-known, however, that tsunami heights are very sensitive to the spatial slip distribution of the seismic source (Geist, 2002; Ruiz et al., 2015). Even after having a finite fault model, the simulation of the tsunami propagation can take several hours depending on the desired level of resolution. This is the reason why the tsunami forecasts of many of the current warning systems are based on pre-computed scenarios (Reymond et al., 2012; Gusman et al., 2014; Mulia et al., 2018). Chile and Japan use this methodology for that purpose (https://www.jma.go.jp/jma/en/News/lists/tsunamisystem2006mar.pdf). This methodology, however, ignores the complexity of the seismic source and solves only for uniform slip models. We propose a methodology applicable to near-field tsunamis triggered by earthquakes that complements the monitoring systems in operation, and helps make better decisions during and after an emergency alert.

2 Methodology

We can separate this problem into three main parts: 1) the estimation of a seismic source model, 2) the generation of initial conditions, and 3) the corresponding tsunami simulation. We define a computation domain around the earthquake source and the coastal areas in the near field. We use the SRTM15 bathymetric data with 15 arcsec of resolution, based on the STM30 (Becker et al., 2009).

The core idea consists in trading off some accuracy to gain speed. Within the context of tectonic tsunamis generated in the near field we want to know the places with the maximum inundation, the extension of the inundation until it decreases to 0.5 to 1 m, and the average runup. Our model does not aim at computing a detailed inundation map with the best possible accuracy, but rather to provide a fast estimate of the main area prone to inundation relying on the W-phase CMT, currently considered one of the fastest and more accurate methods to characterize the source of large earthquake (Kanamori and Rivera, 2008).

2.1 Slip Distribution Model

Once a W-phase solution provides a characterization of an earthquake we use an elliptical slip distribution (Dmowska and Rice, 1986) over a region determined with the scaling laws obtained by Blaser et al. (2010). This serves as a preliminary estimation while seismic waves are still traveling, and later finite fault solutions are computed. This in turn allows to model the near field tsunami for every finite fault model update. The elliptic model is discretized with n_y subfaults along-dip and $n_x = \lceil \frac{L}{W} n_y \rceil$, where L and W are the length and width of the fault plane obtained with the scaling law. With $n_y = 16$, all the studied cases have enough resolution on the source area.

2.2 Tsunami Initial Conditions

Despite evidence of influence of the source time components in the tsunami generation process, for speed purposes we model a static seafloor deformation induced by a non-uniform slip distribution that includes the horizontal components, as suggested in Tanioka and Satake (1996). This is obtained by applying the Okada equations (Okada, 1985).

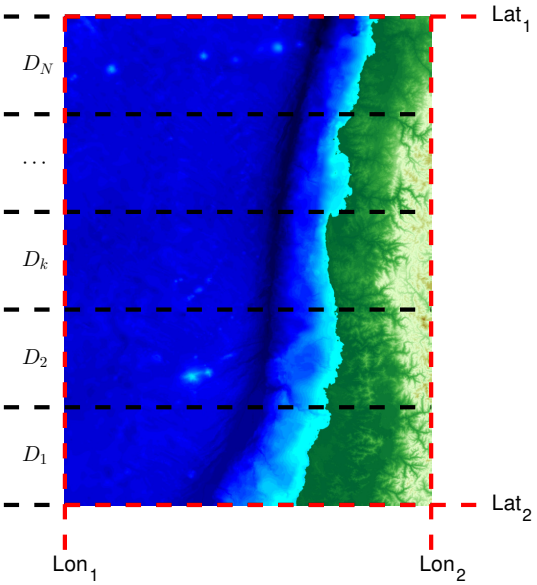

Figure 1. Schematic showing the discretization of the calculation domain for parallel computation.

2.3 Tsunami Modeling

The last part of this methodology is the estimation of the tsunami heights along the coast. Usually, tsunami modeling involves complex codes to solve the fully coupled non-linear shallow water equations. Depending on the domain size and resolution, a full tsunami simulation run can take several hours, which makes real-time forecast nearly impossible. To overcome this limitation, we solve the linear shallow water equations with a forward finite difference scheme. The propagation inside the domain is governed by the second order PDE with initial conditions:

$$\begin{aligned} \eta_{tt} - g\nabla\left(h\nabla\eta\right) &= 0 \\ \eta(x,y,0) &= \eta_0(x,y) \\ \eta_t(x,y,0) &= 0 \end{aligned} \tag{1}$$

where $\eta(x,y,t)$ denotes the water surface, g the acceleration of gravity, $h(x,y)$ the bathymetry and $\eta_0(x,y)$ the initial condition. In the open boundaries, we set a radiation condition (Reid and Bodine, 1968), whereas in the solid boundaries (coasts) we impose full reflection in a vertical wall placed at an isobath of 100 m, before reaching the non-linear zone. Here, a Neumann boundary condition is applied: $\frac{\partial\eta}{\partial\hat{\boldsymbol{n}}}$ where $\hat{\boldsymbol{n}}$ denotes the exterior unit normal vector. The linear method (LM) allows to obtain a quicker estimation than a full tsunami code since second-order terms are disregarded while still accounting for the same main features. In addition, this approach does not require computing the velocity field, an added benefit that makes the computation programs even faster. Each simulation is compared to its corresponding full non-linear shallow water equation propagation. We use the JAGURS code (Baba et al., 2014) written in Fortran90 using parallel arrays via OpenMP and OpenMP

+ MPI. This code is based on the classical finite difference method of Satake (2002). For each scenario, we run the simulation for the equivalent of two hours of tsunami travel time to obtain the main features of the runup distributions, despite the fact that later amplification of edge waves and resonances effects can occur. The approximated runup is obtained as the maximum from the vertical wall reflexion boundary condition. This is usually on the same order with the actual runup in a sloping beach model (Synolakis, 1987).

3 Implementation and Benchmarking

To evaluate the performance of our approach, we modeled nearly all the great tsunamis of the last two decades. Most of them were already tested with an analytical approach in (Riquelme et al, 2015). The details of the propagation and runup distribution of the 12 events tested are presented in the supporting information. For these examples we used the finite fault models provided by the USGS (Hayes, 2017), as they have proven to be operationally robust for real time operations in the context of global monitoring. All the computations were performed in a Dell Precision 7920, with two Intel Xeon Gold 6136 processors, each with 12 physical cores, for a total of 24 physical cores, and 2 threads each. For each time iteration, the domain is divided into 48 subdomains that are computed in different threads, for a parallel array (Fig.1). To compute the tsunami initial condition, the Okada equations were implemented in the C programming language using threading, together with the finite difference scheme for the LM. The C code uses the pthread library to define a C data structure containing a pthread, and then calls a function that sends each grid subdomain to threads running in different cores for computation. This method is as reliable as any other linear scheme method, as it solves the same equations. The only significant difference is in the threads distribution for time optimization. When a thread finishes, it computes for a certain time step and it joins with the others in order to avoid miscomputations. For instance, on the system used to run our computations for a regular grid of 4 million points with an FFM of 300 subfaults, the vertical and horizontal seafloor displacements can be calculated almost instantly (less than 5 seconds), and two hours of tsunami wave propagation for the 2011 Tohoku, Japan earthquake can be solved in 60 seconds.

4 Discussion of Computational Results

All the earthquakes presented here, have produced tsunamis. The range of magnitude varies from 7.7 to 9.1. They occurred in different subduction zones around the world. The largest ones are Tohoku in Japan and Maule in Chile. All of them show a thrust mechanism except for the Samoa event in 2009 which is a normal event. There are a few tsunami earthquakes in this section such as the 1992 Mw 7.7 Nicaragua Earthquake, The 2006 Mw 7.6 Java Earthquake. The extension of the earthquakes varies from $L = 150$ km to $L = 500$ km, the range of peak displacement at the source varies from 3 m to 40 m. Therefore, we have tested as many earthquakes and as many source features as possible for this study.

1. The 1992 Mw 7.7 Nicaragua Tsunami Earthquake
2. The 2001 Mw 8.4 Southern Perú Earthquake

3. The 2003 Mw 8.3 Hokkaido Earthquake
4. The 2006 Mw 7.6 Java Earthquake
5. The 2007 Mw 8.1 Solomon Islands Earthquake
6. The 2007 Mw 8.0 Pisco Earthquake
7. The 2009 Mw 8.1 Samoa Islands Region Earthquake
8. The 2010 Mw 8.8 Maule Earthquake
9. The 2011 Mw 9.0 Tohoku Earthquake
10. The 2012 Mw 7.8 British Columbia Earthquake
11. The 2014 Mw 8.2 Iquique Earthquake
12. The 2015 Mw 8.3 Illapel Earthquake

For each event we apply the methodology previously described, and use the W-phase centroid moment tensor, a scaling law, and an elliptic slip distribution to define the first source. Then, the linear and non-linear tsunami simulations are performed. The resulting runup distributions are decomposed along latitude and longitude in order to compare both models. The same procedure is repeated, this time considering an FFM solution instead. Table 1 shows the correlation between the runup distributions obtained with the JAGURS code (non-linear method) and the method presented in this paper (linear method). Table 2 summarizes the CPU times in seconds for different stages of the process for each simulation. There is a high degree of agreement within a short time. Detailed figures showing the results for the 24 simulations are provided in the supplementary material, where maximum amplitudes, runup distribution, and field measurements are listed. For comparison purposes, the event of 2014 Chile, the DART station 32401 registered 0.25 m of amplitude (An et al., 2014), where the linear method predicts 0.39 m for the elliptic source and 0.12 m for the FFM, whereas JAGURS gives 0.55 m for the elliptic source and 0.15 m for the FFM.

5 Application to compliment tsunami alert. Case study: The 2015 Illapel Earthquake

On 16 September, 2017 an 8.3 Mw earthquake occurred in the Coquimbo region, Chile (Melgar et al., 2016; Fuentes et al., 2017). The characteristics of this event made it an ideal case study for tsunami generation. The national agencies implemented the established protocols for evacuating the whole Chilean coast, even the more distant insular territories (SNAM, bulletin 1, Sept. 16th, 23:02 5 UTC). Such decisions have to be made within minutes of origin time. In general, an accurate prediction of the tsunami runup heights requires a precise image of the seismic source, which at present is not available within 5 minutes for real-time after adding the tsunami simulation times. Nevertheless, we can come close to a quasi-real-time approach by triggering a first estimation assuming an elliptical slip distribution. This only takes a few seconds, and can at present be done instead of searching a pre-computed database of scenarios that are usually limited. For monitoring purposes, the results can

Table 1. Correlation of the runup distribution obtained from our linear model solution and the JAGURS code. Correlation is computed with the standard Pearson coefficient. Details can be found in the supplemental material.

Event	FFM lon	FFM lat	Elliptic lon	Elliptic lat
1992 Nicaragua	0.8323	0.8088	0.8841	0.8587
2001 Perú	0.8334	0.8575	0.6697	0.7549
2003 Japan	0.7753	0.7838	0.9139	0.9129
2006 Indonesia	0.7483	0.8531	0.8134	0.9030
2007 Solomon Isl.	0.6422	0.7575	0.8412	0.8626
2007 Perú	0.8380	0.8085	0.8872	0.8896
2009 Samoa	0.6987	0.7353	0.7779	0.8093
2010 Chile	0.7346	0.6039	0.8682	0.7820
2011 Japan	0.8571	0.7074	0.9229	0.8311
2012 Canada	0.6829	0.6034	0.8731	0.8398
2014 Chile	0.7833	0.6473	0.9051	0.8341
2015 Chile	0.9103	0.7663	0.9603	0.8686

Table 2. Summary of the CPU time in seconds for the twelve events. t_{IC} indicates the time needed to compute the initial conditions, t_{Pr} the processing time, t_{TP} the time to compute the tsunami propagation, and t_T the total time.

Event	FFM		Elliptic		LM	JAGURS	Total time t_T			
	t_{IC}	t_{Pr}	t_{IC}	t_{Pr}	t_{TP}	t_{TP}	FFM-LM	FFM-JAGURS	Elliptic-LM	Elliptic-JAGURS
1992 Nicaragua	6	4	8	5	31	575	41	585	44	586
2001 Perú	5	3	7	3	18	360	26	368	28	370
2003 Japan	5	3	9	3	22	428	30	436	34	440
2006 Indonesia	4	3	7	2	20	358	27	365	29	367
2007 Solomon Isl.	8	5	10	5	28	658	41	671	43	673
2007 Perú	4	4	9	4	31	546	39	554	44	559
2009 Samoa	4	3	6	2	17	321	24	328	25	329
2010 Chile	7	4	9	5	32	651	43	662	46	665
2011 Japan	6	6	13	6	46	223	58	235	65	242
2012 Canada	2	1	4	1	15	153	18	156	20	158
2014 Chile	5	4	11	5	24	500	33	509	40	516
2015 Chile	4	4	8	4	27	500	35	508	39	512

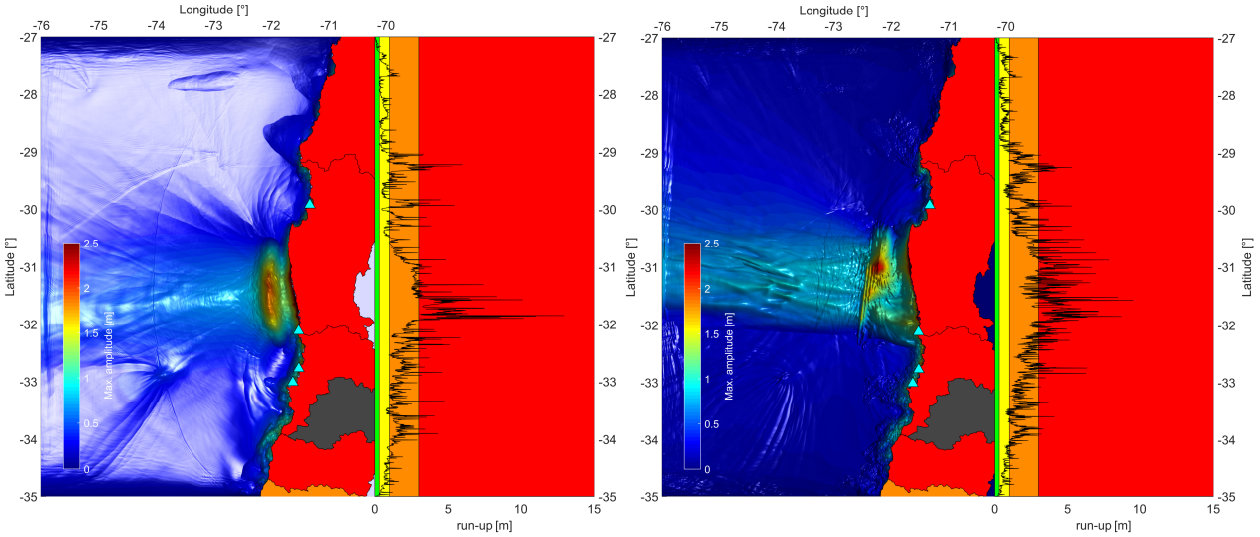

Figure 2. Near field simulation of the 2015 Illapel earthquake with an elliptical source (left), and a finite fault model (right). The colors assigned to different areas indicate the expected runups in meters: a) red for runups larger than 3 m, b) orange for runups between 1 and 3 m, c) yellow for runups between 0.3 and 1 m, and d) green for runups smaller than 0.3 m.

be updated everytime a seismic source imaging is received, for both, the near field (at 15 arcsec) and regional field (at 60 arcsec). All this information is summarized in a color-coded map following the official coding used by the Chilean institutions (Melgar et al., 2016). Color coded maps are self-explanatory, which makes them easy to interpret (Figs.2 and 3). Each region can then be rapidly assigned a color linked to an specific evacuation protocol. All the simulations were performed for two hours of tsunami propagation where the main energy content plays a key role on the inundation process. Figure 4 illustrates the normalized energy rate that generates the runup history along the coast, showing that the majority of the global energy is concentrated within the first hour. We can also observe that the first estimation obtained for an elliptical fault predicts the same levels of inundation as the full finite fault model in the near field, while we can observe minor differences in the regional field. This makes sense since finite fault model results become available during the tsunami monitoring stage, when time is not as critical as in the very first minutes after origin time. It has to be noticed that is possible to increase the number of warning levels allowing to find the optimal number of states for emitting and communicating the warning bulletin. In this study we choose the UNESCO standard. For completeness, we computed the travel time isochrones across the Pacific Basin (Fig. 5). These computations use a dense set of rays following Sandanbata et al. (2018), which allows to include dispersive effects. We have also included the effect of the earth elasticity as shown in An and Liu (2016). These kind of maps can be computed instantly together with the very first estimation of the moment tensor and then updated.

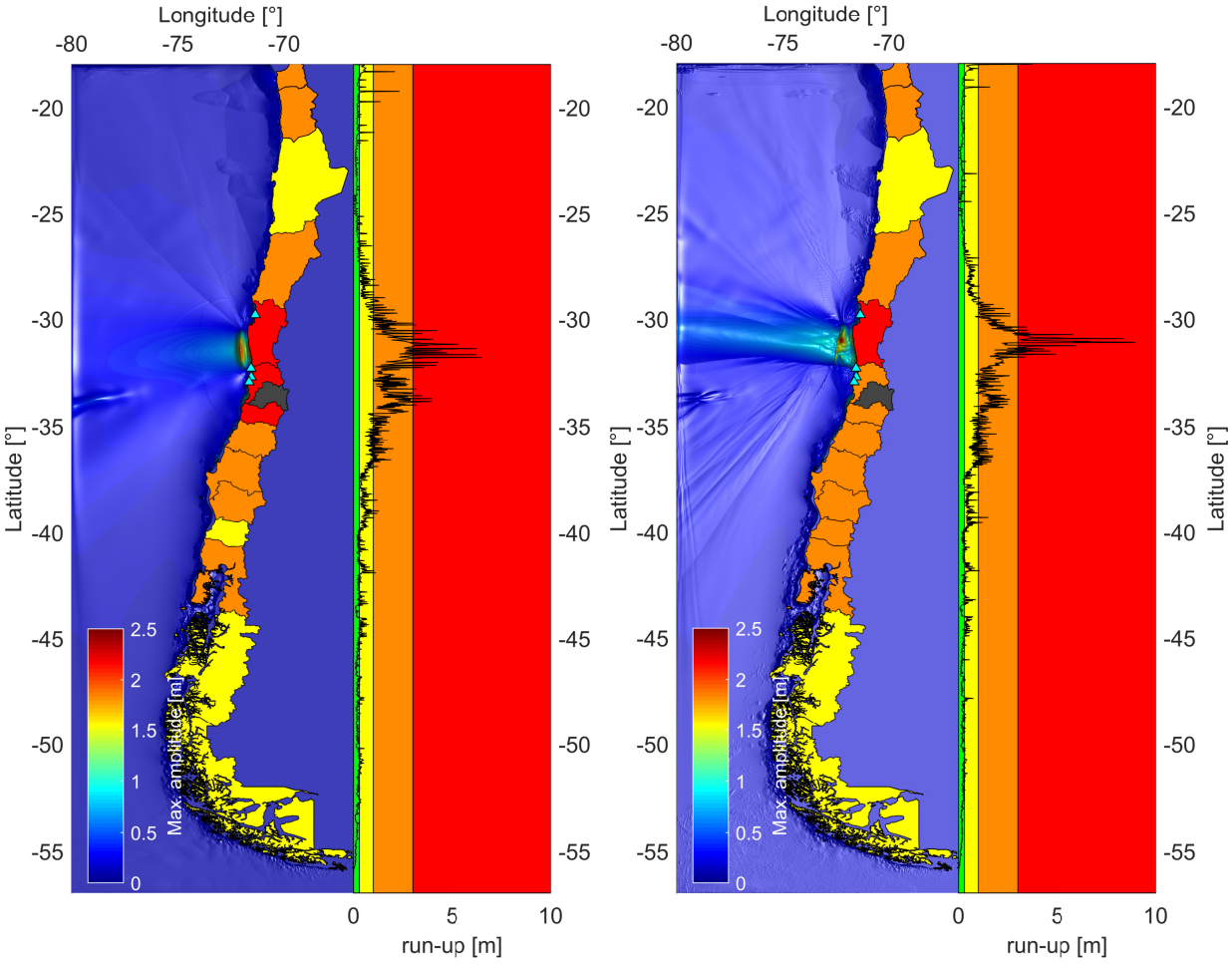

Figure 3. Regional field simulation of the 2015 Illapel earthquake for an elliptical source (left), and a finite fault model (right). The colors assigned to different areas indicate the expected runups in meters: a) red for runups larger than 3 m, b) orange for runups between 1 and 3 m, c) yellow for runups between 0.3 and 1 m, and d) green for runups smaller than 0.3 m.

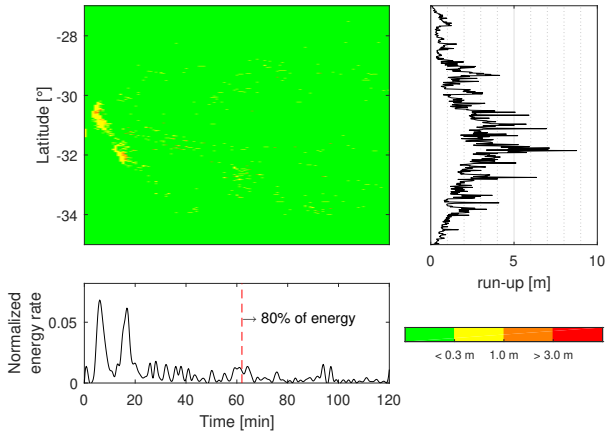

Figure 4. Normalized runup energy rate during the first two hours of tsunami simulation. The upper left panel shows the runup rate along latitude and time, the upper right panel shows the final maximum runup, and the bottom left panel shows the normalized energy rate for the whole process as a time series.

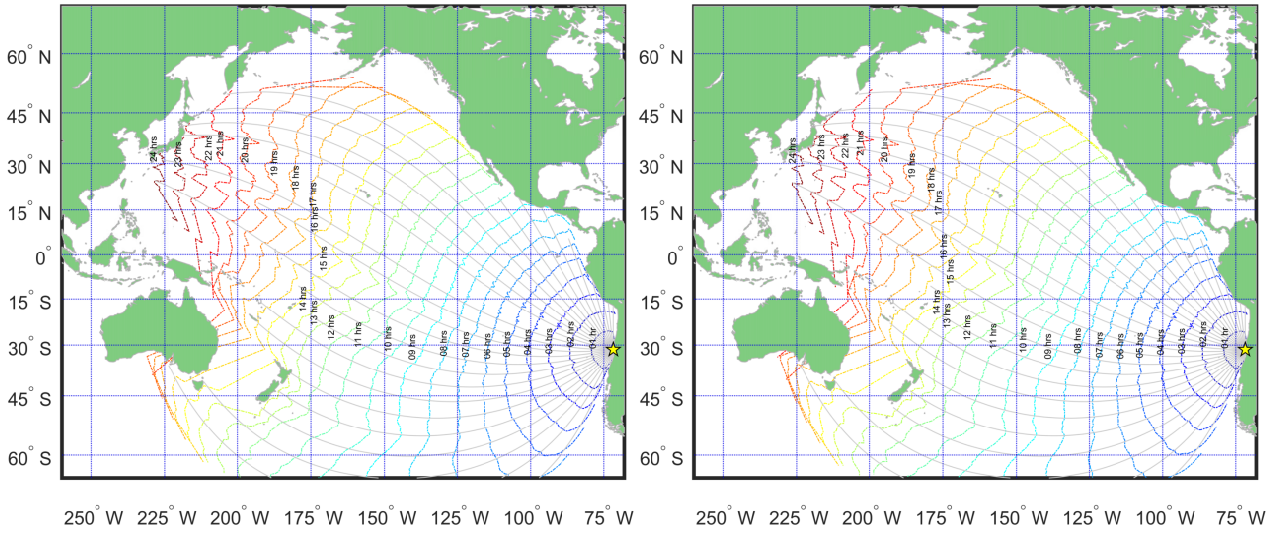

Figure 5. Tsunami travel times across the Pacific basin for the 2015 Illapel earthquake.The left panel shows the travel times after the shallow water equations, while the travel times in the right panel include the effects of dispersion and the earth elasticity for a wave frequency of 2 mHz.

6 Conclusions

In this study we propose a method that disregards the fine complexity of the seismic source while using fine bathymetric data and a set of simplified equations to model more than 80% of the runups with enough accuracy for tsunami warning purposes up

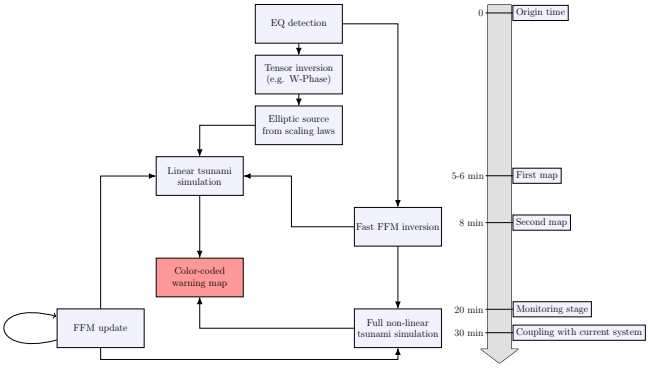

Figure 6. Flow chart of the methodology proposed in this study.

to 20 times faster. Our method also aims at rapidly predicting the spatial distribution of the runups using some simplifications in the tsunami equations. Despite lacking the mathematical rigorosity that we would otherwise prefer, the method we propose is not inexact within the context of an emergency response system that needs to trigger actions that can potentially save lives and reduce economic losses after the occurrence of a large earthquake. We summarized our approach in a flow chart (Fig. 6). Taking into account the results of our study we can list the following as the most noteworthy results:

1. Although other tsunami warning centers use linear theory as part of their operations, for instance at the PTWC (http://unesdoc.unesco.org/images/0022/002203/220368e.pdf), in this study we have combined it with the use of more complex sources and faster algorithms to generate a unique and simple product easy to interpret.

2. The non-complexity of the adopted source does not seem to significantly affect the results of a fast runup estimation for emergency response purposes. By computing different levels of tsunami hazard in near-real time we estimate more accurately the extent of the area potentially affected by the tsunami, the maximum level of inundation, and how many people will be exposed to this hazard along the Chilean coast.

3. Using the methodology of Sandanbata et al. (2018) it is possible to instantaneously calculate the tsunami arrival times from sources generated in the far field with enough accuracy. This can also be done via tsunami modeling, but at the expense of longer computation times.

4. When compared to other tsunami modeling codes such as JAGURS, results obtained from our method match more than 80% of the predicted runup for 15 arcsec bathymetry while obtaining the results at least 20 times faster.

5. The simple method proposed in this study provides a fast, reliable, and intuitive characterization of the tsunami threat, which in turn allows disaster mitigation agencies to take appropriate action.

Acknowledgements. This study was enterally supported by the *Programa de Riesgo Sśmico*.

References

AN, C., SEPÚLVEDA, I., AND LIU, P. L. F. *Tsunami source and its validation of the 2014 Iquique, Chile, earthquake.* Geophysical Research Letters, 41(11), 3988-3994, 2014.

AN, C., AND LIU, P. L.: *Analytical solutions for estimating tsunami propagation speeds*, Coastal Engineering, 117, 44-56, 2016.

BABA, T., TAKAHASHI, N., KANEDA, Y., INAZAWA, Y., KIKKOJIN, M.: *Tsunami Inundation Modeling of the 2011 Tohoku Earthquake Using Three-Dimensional Building Data for Sendai, Miyagi Prefecture, Japan.*, In: Kontar Y., Santiago-Fandiño V., Takahashi T. (eds) Tsunami Events and Lessons Learned. Advances in Natural and Technological Hazards Research, 35. Springer, Dordrecht, 2014.

BECKER, J. J., SANDWELL, D. T., SMITH, W. H. F., BRAUD, J., BINDER, B., DEPNER, J., FABRE, D., FACTOR, J., INGALLS, S., KIM, S-H., LADNER, R.,MARKS, K., NELSON, S., PHARAOH, A., SHARMAN, G., TRIMMER, R., VON ROSENBURG, J., WALLACE G., AND WEATHERALL, P.: *Global bathymetry and elevation data at 30 arc seconds resolution: SRTM30_PLUS*, Marine Geodesy, 32(4), 355-371, 2009.

BLASER, L., KRÜGER, F., OHRNBERGER, M., AND SCHERBAUM, F.: *Scaling relations of earthquake source parameter estimates with special focus on subduction environment*, Bulletin of the Seismological Society of America, 100(6), 2914-2926, 2010.

DOI, K.: *Tsunami Warning System in Japan*, In: Zschau J., Küppers A. (eds) Early Warning Systems for Natural Disaster Reduction. Springer, Berlin, Heidelberg, 2003.

DMOWSKA, R., AND RICE, J. R.: *Fracture theory and its seismological applications*, Continuum Theories in Solid Earth Physics, 3, 187-255, 1986.

FUENTES, M., RIQUELME, S., HAYES, G., MEDINA, M., MELGAR, D., VARGAS, G., GONZALEZ, J., AND VILLALOBOS, A.: *A study of the 2015 Mw 8.3 Illapel earthquake and tsunami: Numerical and analytical approaches*, In The Chile-2015 (Illapel) Earthquake and Tsunami, 255-266. Birkhäuser, Cham, 2017.

GEIST, E. L.: *Complex earthquake rupture and local tsunamis*, Journal of Geophysical Research: Solid Earth, 107(B5), 2002.

GUSMAN, A.R., TANIOKA, Y., MACINNES, B.T. AND TSUSHIMA, H.: *A methodology for near-field tsunami inundation forecasting: Application to the 2011 Tohoku tsunami*, J. GEOPHYS. RES.: SOLID EARTH, 119(11), 8186-8206, 2014.

HAYES, G.: *The finite, kinematic rupture properties of great-sized earthquakes since 1990*, EARTH AND PLANETARY SCIENCE LETTERS 468, 94-100, 2017.

IDE, S., BEROZA, G. C., SHELLY, D. R., AND UCHIDE, T.: *A scaling law for slow earthquakes*, NATURE, 447(7140), 76-79, 2007.

KANAMORI, H., AND RIVERA, L.: *Source inversion of Wphase: speeding up seismic tsunami warning*, GEOPHYSICAL JOURNAL INTERNATIONAL, 175(1), 222-238, 2008.

MELGAR, D., ALLEN, M., RIQUELME, S., GENG, J., LIANG, C., BRAVO, F., BAEZ, J.C., PARRA, H., BARRIENTOS, S., PENG, F., BOCK, Y., BEVIS, M., CACCAMISE, DANA., VIGNY, C., MORENO, M., AND SMALLEY, R.: *Local tsunami warnings: Perspectives from recent large events.*, GEOPHYSICAL RESEARCH LETTERS, 43(3), 1109-1117, 2016.

MULIA, I. E., GUSMAN, A. R., AND SATAKE, K.: *Alternative to non-linear model for simulating tsunami inundation in real-time*. GEOPHYSICAL JOURNAL INTERNATIONAL, 214(3), 2002-2013, 2018.

OKADA, Y.: *Surface deformation due to shear and tensile faults in a half-space*, BULLETIN OF THE SEISMOLOGICAL SOCIETY OF AMERICA, 75(4), 1135-1154, 1985.

REID, R. O., AND BODINE, B. R.: *Numerical model for storm surges in Galveston Bay*, JOURNAL OF THE WATERWAYS AND HARBORS DIVISION, 94(1), 33-58, 1968.

REYMOND, D., OKAL, E. A., HÉBERT, H., AND BOURDET, M. *Rapid forecast of tsunami wave heights from a database of pre-computed simulations, and application during the 2011 Tohoku tsunami in French Polynesia*. GEOPHYSICAL RESEARCH LETTERS, 39(11), 2012.

RIQUELME, S., FUENTES, M., HAYES, G. P., AND CAMPOS, J.: *A rapid estimation of near-field tsunami runup*, JOURNAL OF GEOPHYSICAL RESEARCH: SOLID EARTH, 120(9), 6487-6500, 2015.

RIQUELME, S., BRAVO, F., MELGAR, D., BENAVENTE, R., GENG, J., BARRIENTOS, S., AND CAMPOS, J.: *W phase source inversion using high-rate regional GPS data for large earthquakes*, GEOPHYSICAL RESEARCH LETTERS, 43(7), 3178-3185, 2016.

RIQUELME, S., MEDINA M., BRAVO, F., BARRIENTOS, S., CAMPOS, J. AND CISTERNAS A.: *W-phase Real Time Implementation and Network Expansion: The Experience in Chile 2012-2017s*, SEISMOLOGICAL RESEARCH LETTERS, 89(6), 2237-2248, 2018.

RUIZ, J. A., FUENTES, M., RIQUELME, S., CAMPOS, J., AND CISTERNAS, A.: *Numerical simulation of tsunami runup in northern Chile based on non-uniform k-2 slip distributions*, NATURAL HAZARDS, 79(2), 1177-1198, 2015.

SATAKE, K.: *Tsunamis*, IN: LEE WHK, KANAMORI H, JENNINGS PC, KISSLINGER C (EDS) INTERNATIONAL HANDBOOK OF EARTHQUAKE AND ENGINEERING SEISMOLOGY, VOL 81A. ACADEMIC, AMSTERDAM, 437-451, 2002.

SYNOLAKIS, C. E. *The runup of solitary waves*. JOURNAL OF FLUID MECHANICS, 185, 523-545.

TANIOKA, Y., AND SATAKE, K.: *Tsunami generation by horizontal displacement of ocean bottom*, GEOPHYSICAL RESEARCH LETTERS, 23(8), 861-864, 1996.

SANDANBATA, O., WATADA, S., SATAKE, K., FUKAO, Y., SUGIOKA, H., ITO, A., AND SHIOBARA, H.: *Ray Tracing for Dispersive Tsunamis and Source Amplitude Estimation Based on Green's Law: Application to the 2015 Volcanic Tsunami Earthquake Near Torishima, South of Japan*, PURE AND APPLIED GEOPHYSICS, 175(4), 1371-1385, 2018.

WÄCHTER, J., BABEYKO, A., FLEISCHER, J., HÄNER, R., HAMMITZSCH, M., KLOTH, A., AND LENDHOLT, M.: *Development of tsunami early warning systems and future challenges*, NATURAL HAZARDS AND EARTH SYSTEM SCIENCES, 12(6), 1923-1935, 2012.

Supporting Information for

Speeding up Tsunami Forecasting to boost Tsunami Warning in Chile

Fuentes, M[(1)]., Arriola S[(2)]., Riquelme, S[(2)]., and Delouis, B[(3)].

(1) Department of Geophysics, Faculty of Physical and Mathematical Sciences, University of Chile
(2) National Seismological Center, Faculty of Physical and Mathematical Sciences, University of Chile
(3) Géoazur, Université de Nice Sophia Antipolis, Observatoire de la Côte d'Azur

Contents of this file
Figures S1 to S24 and Table S1.

S.1 Elliptic sources data

Table S1: List of W-Phase CMT parameters for the tested events.

Event	Lat [°]	Lon [°]	Depth [km]	Strike[°]	Dip[°]	Rake [°]	Moment [Nm]	Mw
1992 Nicaragua	11.26	-87.7258	11.5	293.1	11.7	73.5	4.55E+27	7.71
2001 Perú	-17.06	-73.015	23.5	315.3	16.4	70.4	4.94E+28	8.4
2003 Japan	42.21	143.7746	23.5	245.6	15.6	125.3	2.21E+28	8.16
2006 Indonesia	-9.284	107.419	11.5	284.1	9	86.5	4.11E+27	7.68
2007 Solomon Isl.	-13.79	-76.6	25.5	324.2	14	63.4	2.24E+28	8.17
2007 Perú	-7.86	156.3325	21.5	322.4	30	101.3	1.75E+28	8.09
2009 Samoa	-15.29	-171.9962	15.5	306.5	22.1	-115.3	1.85E+28	8.11
2010 Chile	-35.95	-72.71	30.5	2.3	23.5	79	2.26E+29	8.71
2011 Japan	37.92	143.113	19.5	196.3	11.9	85.5	4.26E+29	9.02
2012 Canada	52.47	-132.13	15	320	29	111	5.18E+27	7.7
2014 Chile	-19.6097	-70.7691	25	328.3	16.9	70.2	2.35E+28	8.14
2015 Chile	-31.38	-71.77	25.5	358	11.5	107.1	3.19E+28	8.23

S.2 Scenarios tested

This section provides 24 figures that resumes the tsunami simulation of each event ($\times$ 12) with an elliptic patch and a finite fault model for both, JAGURS code and the simple linear method presented in this work. The left panel shows the source model, yellow triangles are the DART buoys (when available) and white curve is the isobath of 100 m. The central panel displays the maximum tsunami amplitudes with the linear method and above and right are the corresponding run-up heights along longitude and latitude respectively.

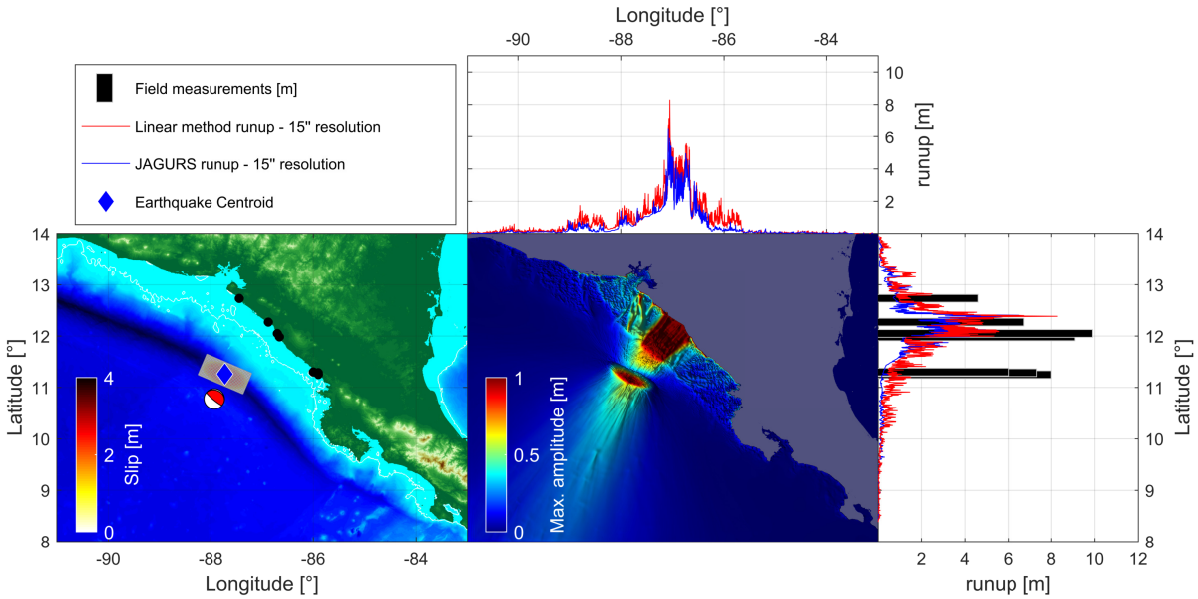

Fig. S1: Summary of the tsunami simulation for The 1992 Nicaragua Earthquake with an elliptic source.

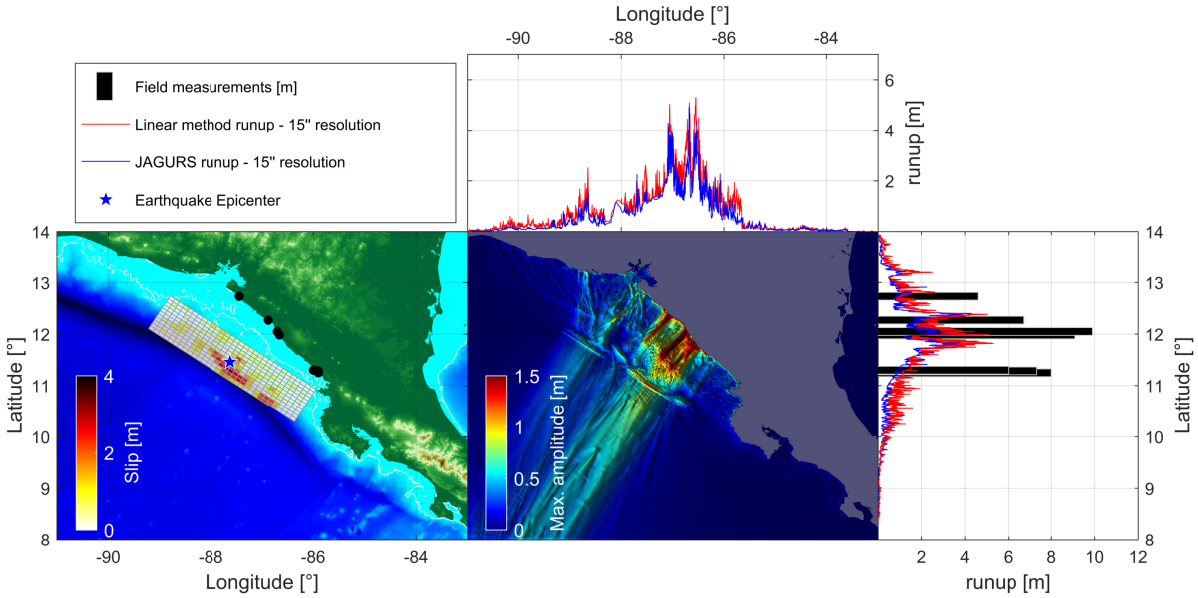

Fig. S2: Summary of the tsunami simulation for The 1992 Nicaragua Earthquake with a finite fault model.

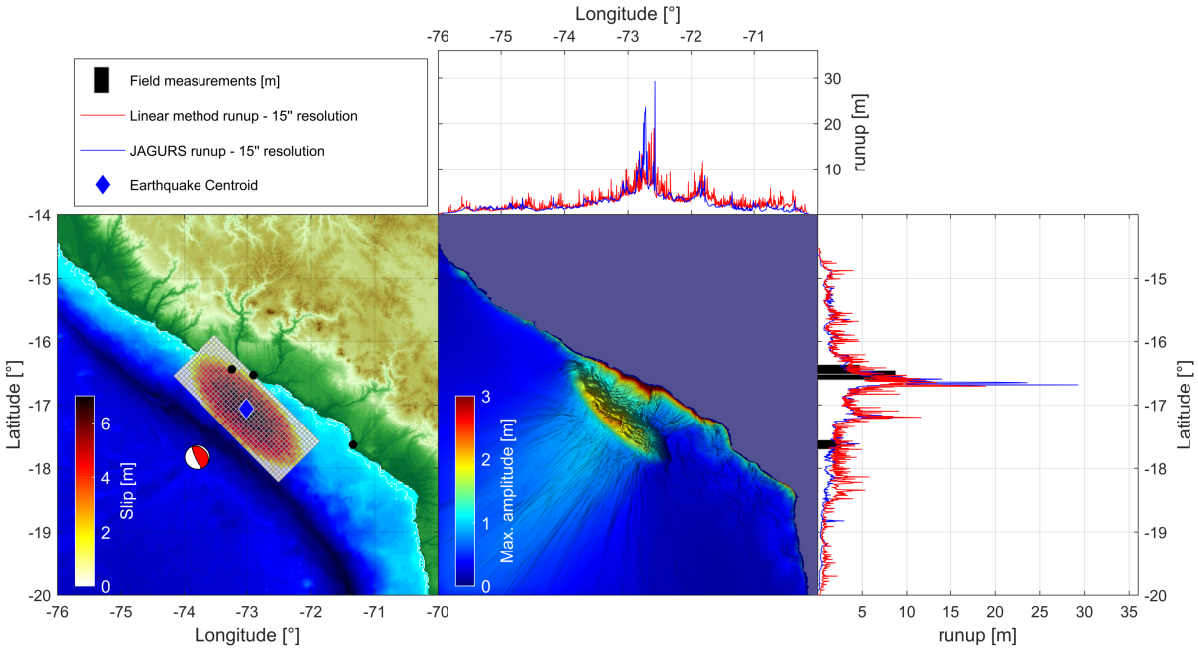

Fig. S3: Summary of the tsunami simulation for The 2001 Southern Perú Earthquake with an elliptic source.

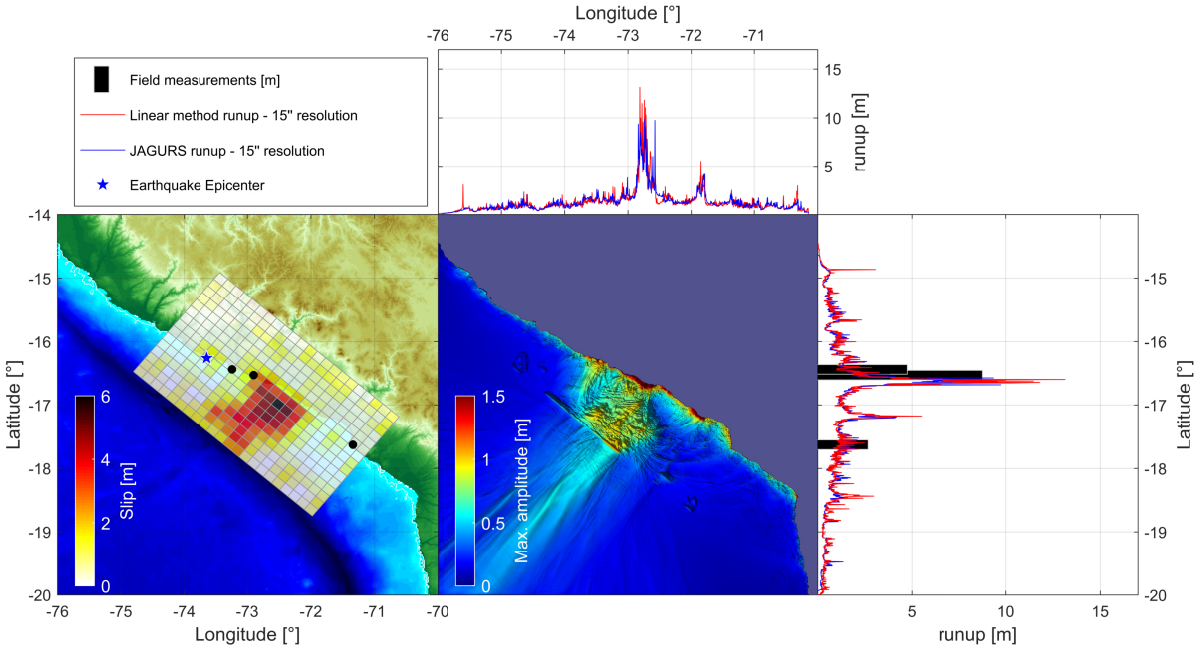

Fig. S4: Summary of the tsunami simulation for The 2001 Southern Perú Earthquake with a finite fault model.

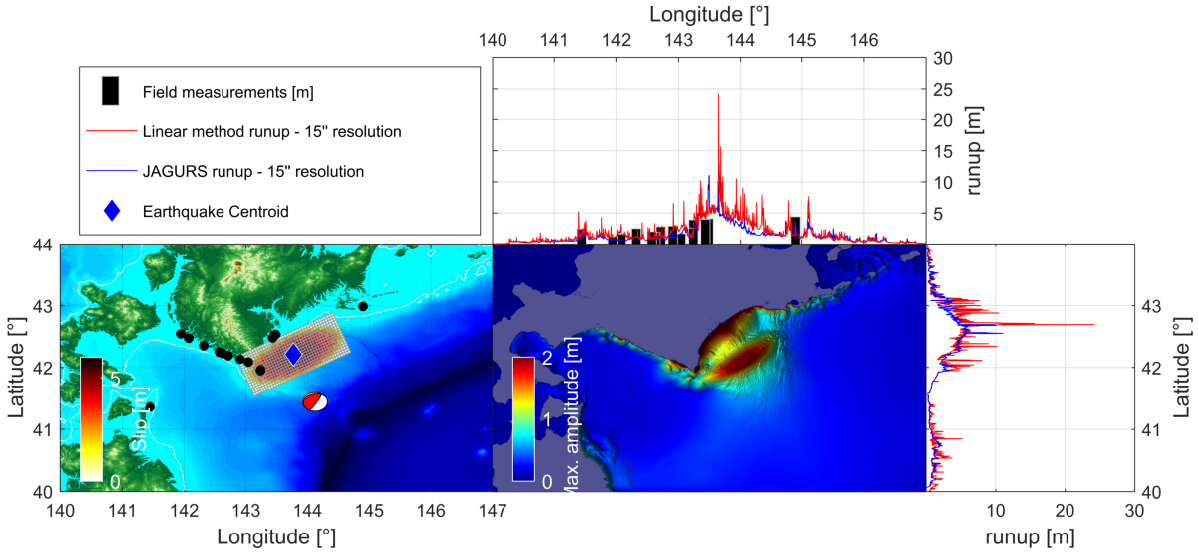

Fig. S5: Summary of the tsunami simulation for The 2003 Japan Earthquake with an elliptic source.

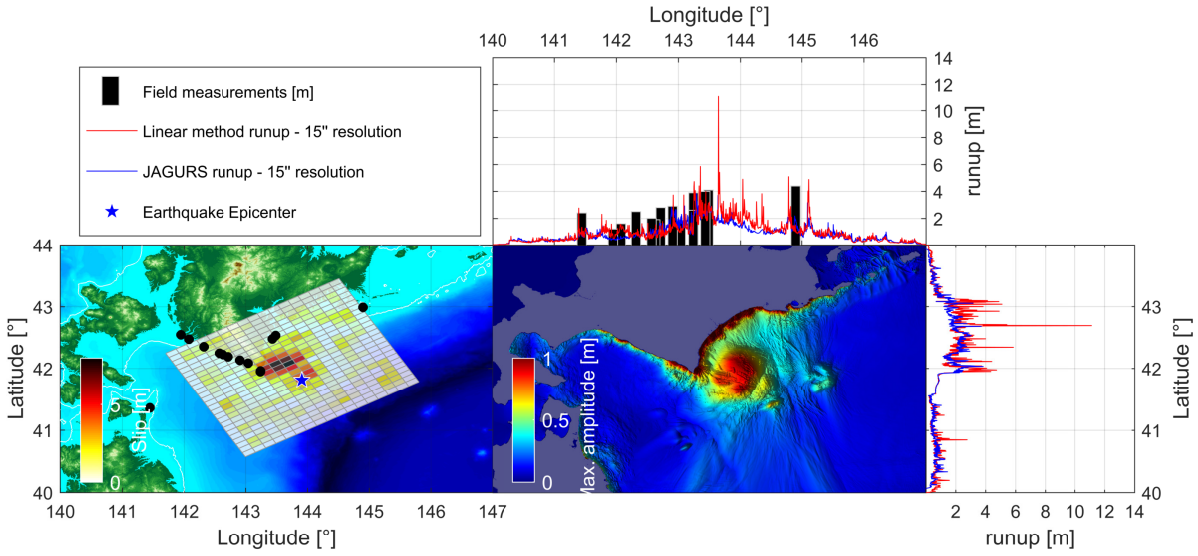

Fig. S6: Summary of the tsunami simulation for The 2003 Japan Earthquake with a finite fault model.

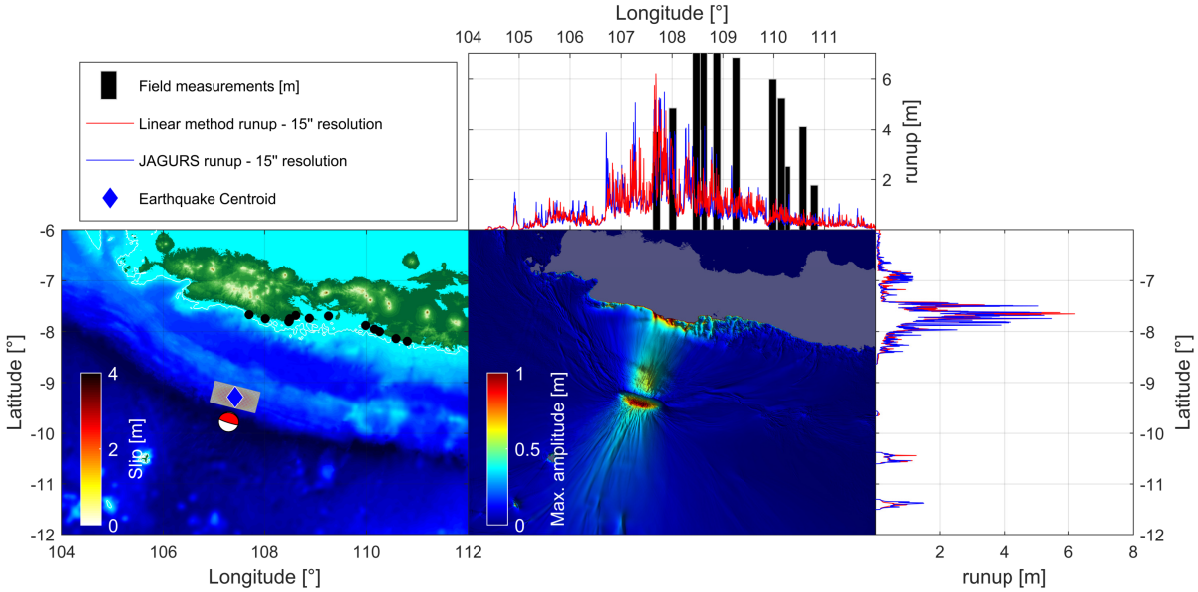

Fig. S7: Summary of the tsunami simulation for The 2006 Indonesia Earthquake with an elliptic source.

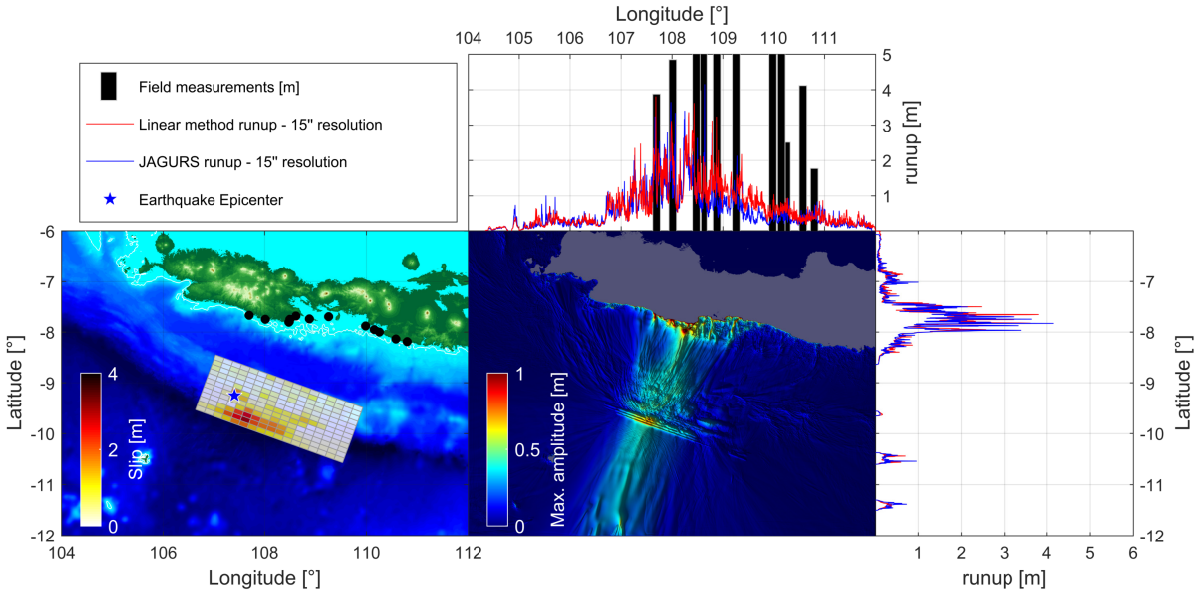

Fig. S8: Summary of the tsunami simulation for The 2006 Indonesia Earthquake with a finite fault model.

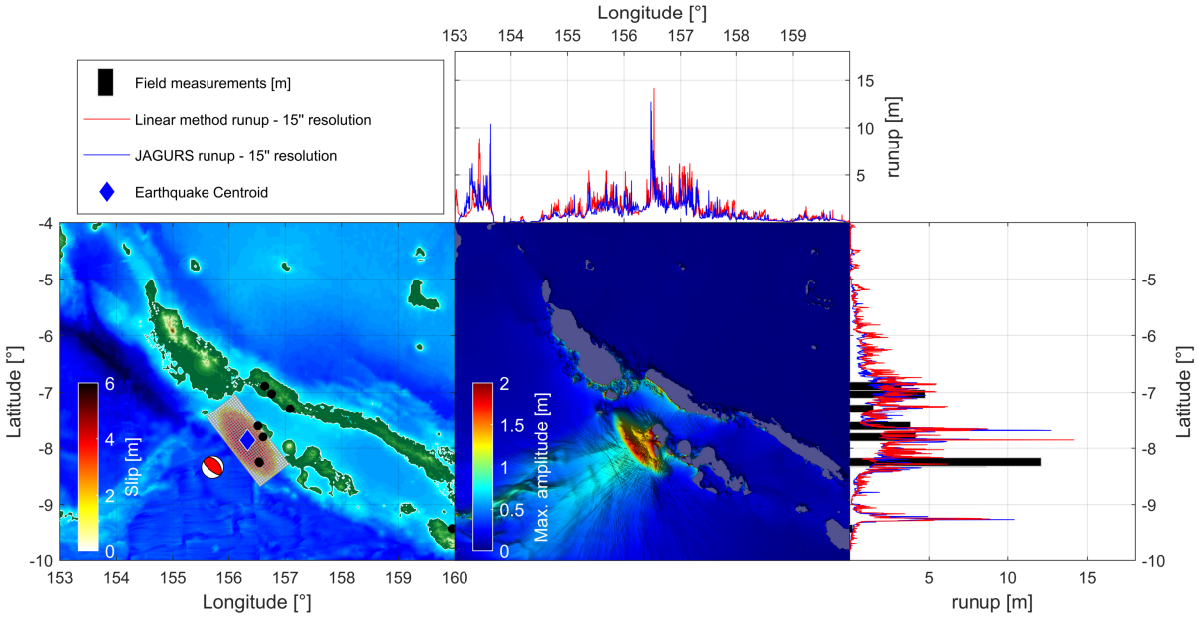

Fig. S9: Summary of the tsunami simulation for The 2007 Solomon Isl. Earthquake with an elliptic source.

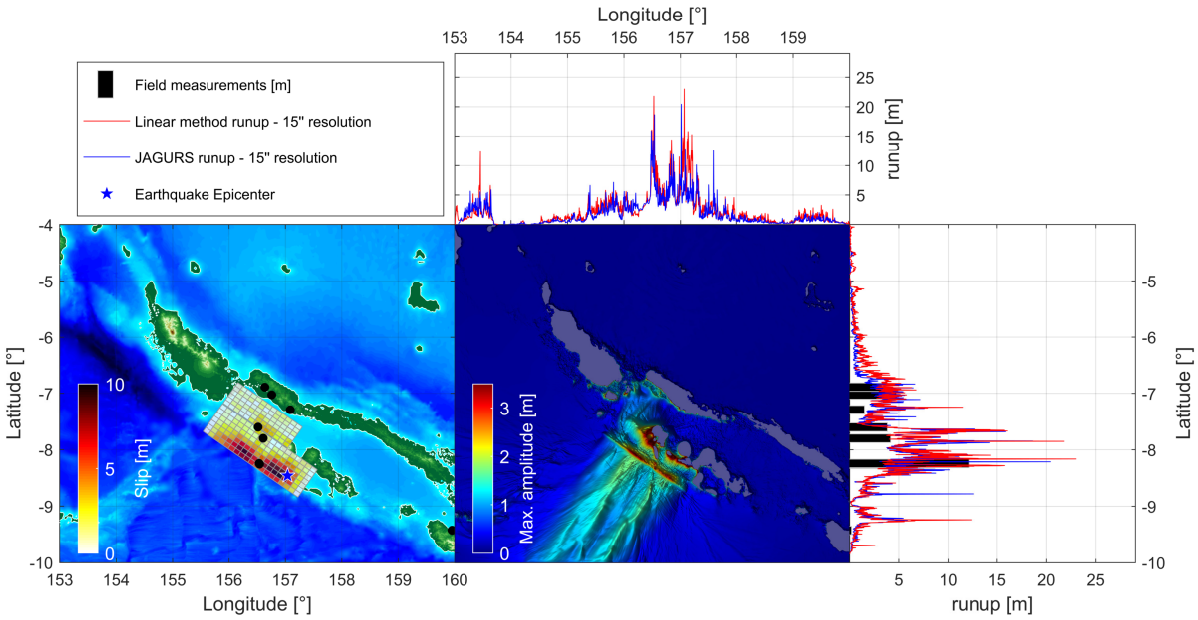

Fig. S10: Summary of the tsunami simulation for The 2007 Solomon Isl. Earthquake with a finite fault model.

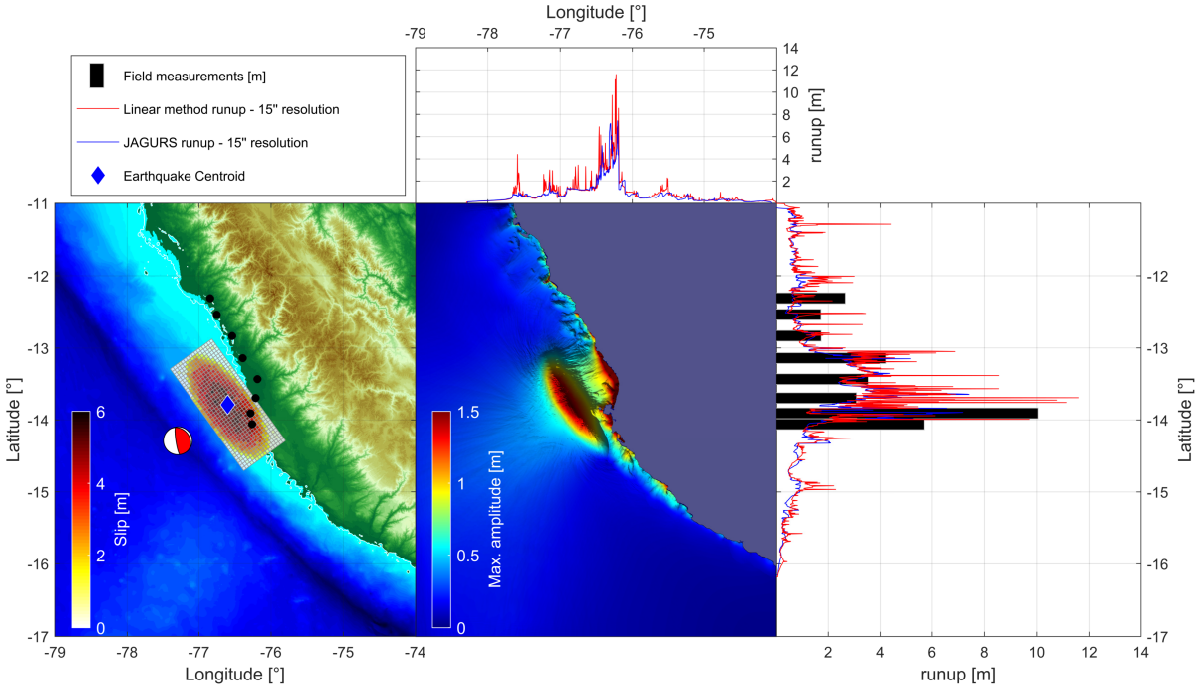

Fig. S11: Summary of the tsunami simulation for The 2007 Perú Earthquake with an elliptic source.

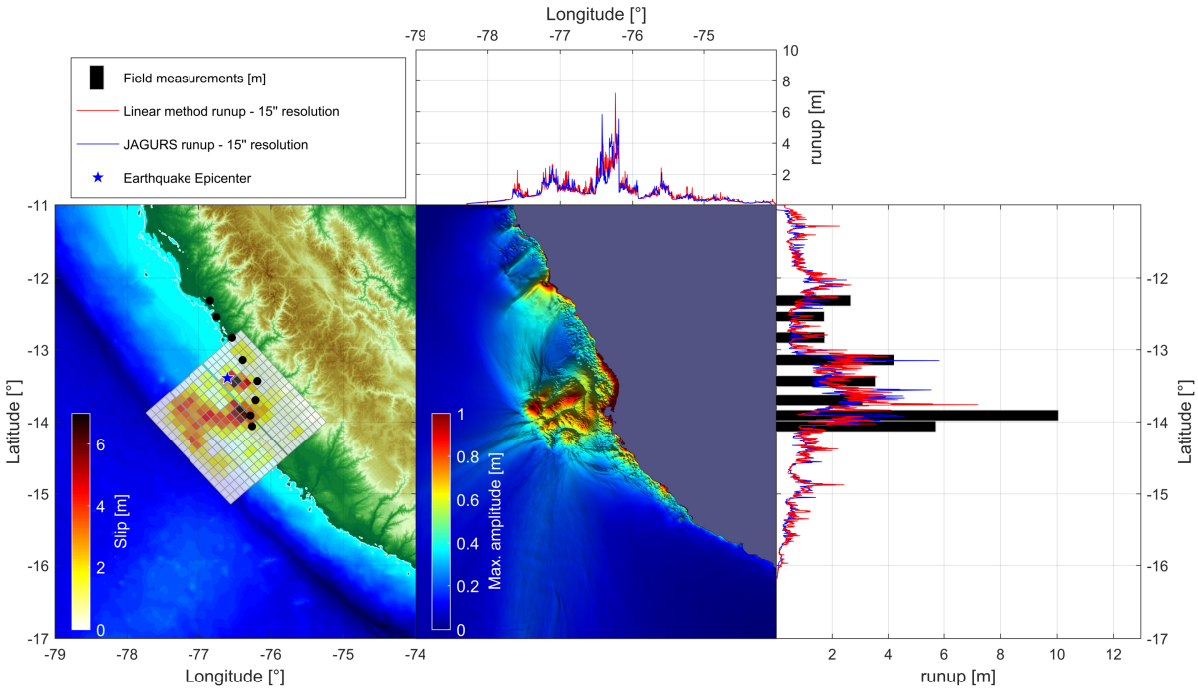

Fig. S12: Summary of the tsunami simulation for The 2007 Perú Earthquake with a finite fault model.

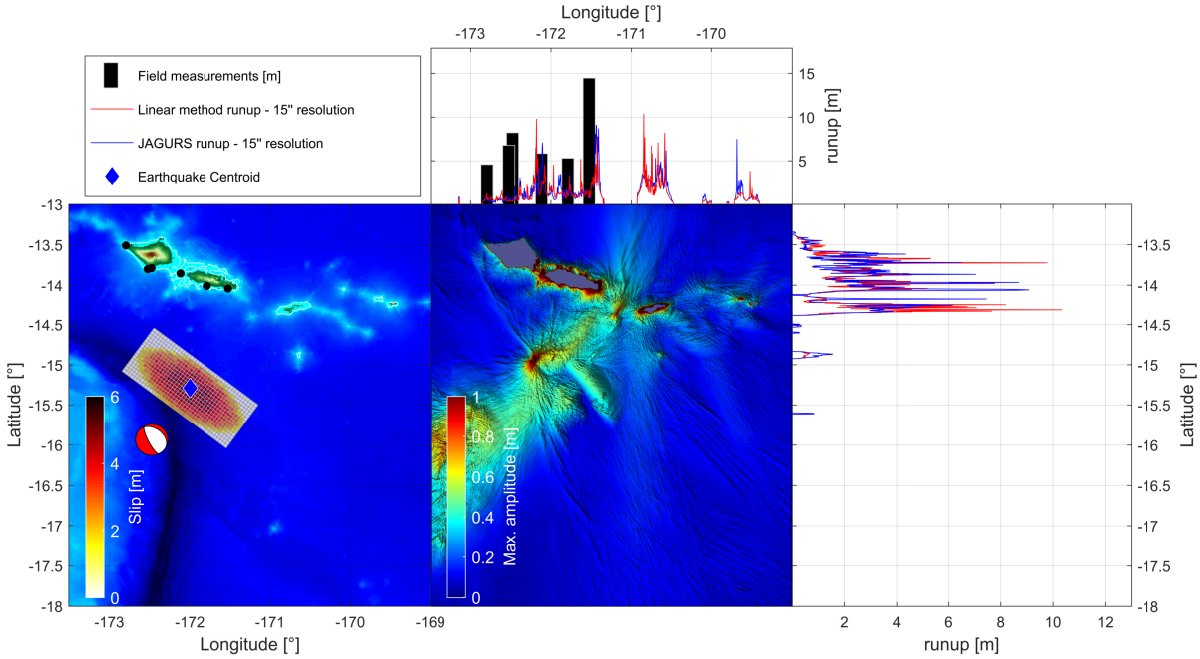

Fig. S13: Summary of the tsunami simulation for The 2009 Samoa Earthquake with an elliptic source.

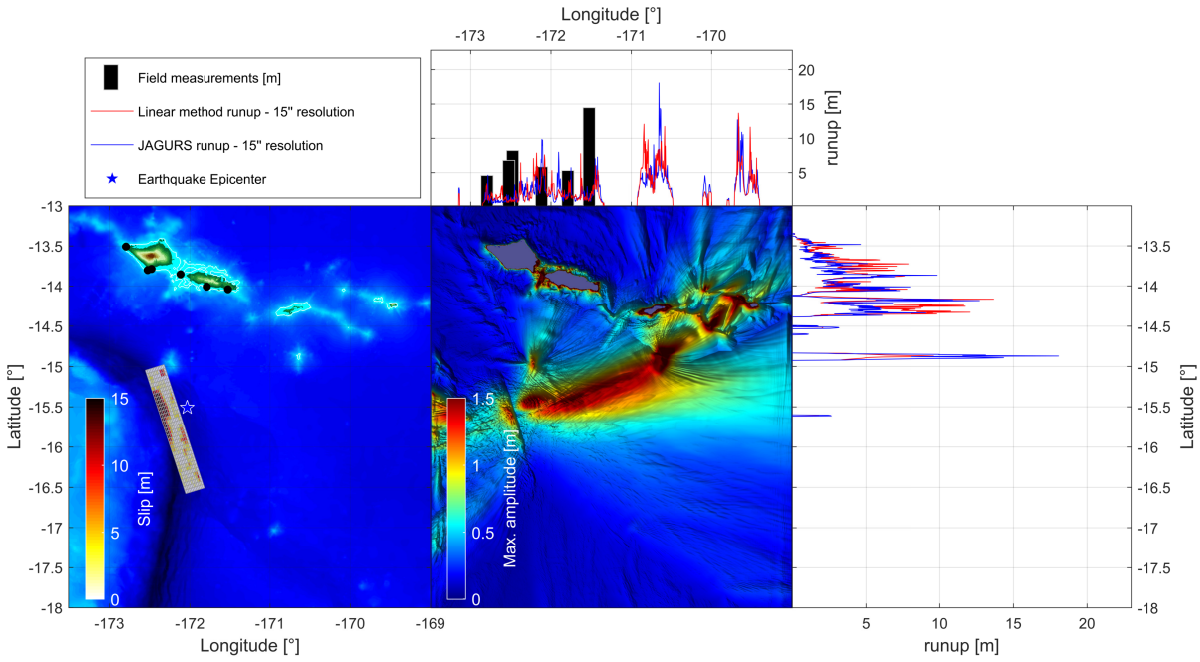

Fig. S14: Summary of the tsunami simulation for The 2009 Samoa Earthquake with a finite fault model.

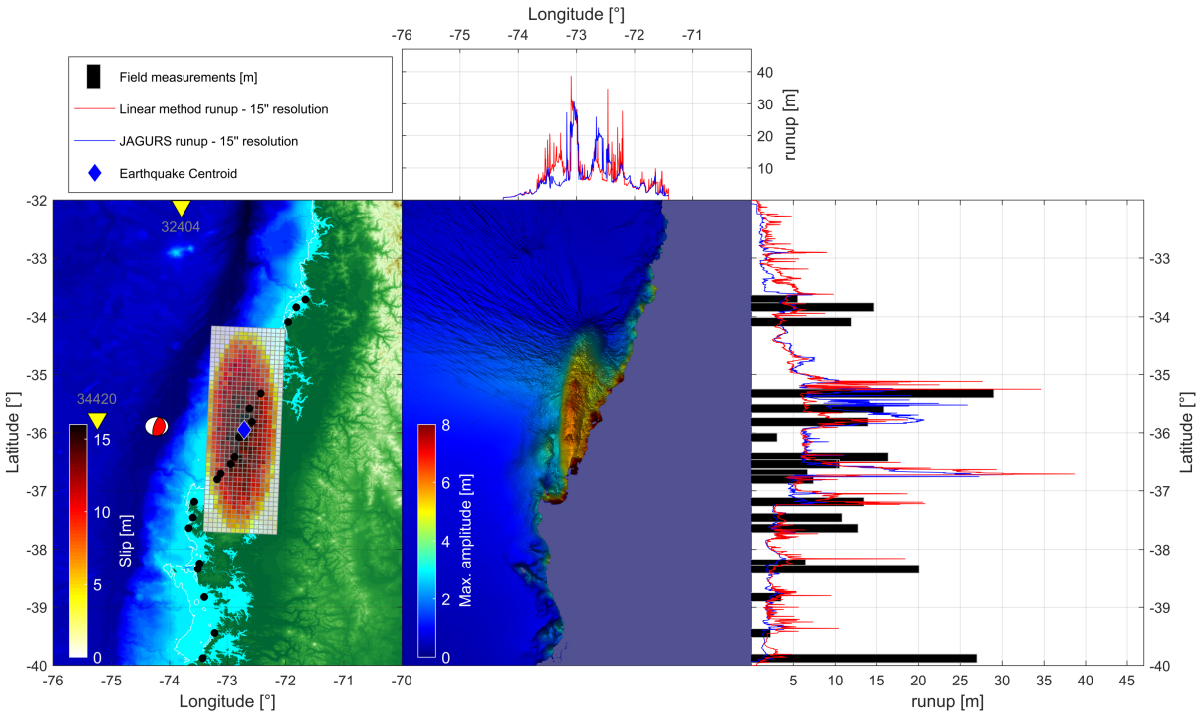

Fig. S15: Summary of the tsunami simulation for The 2010 Chile Earthquake with an elliptic source.

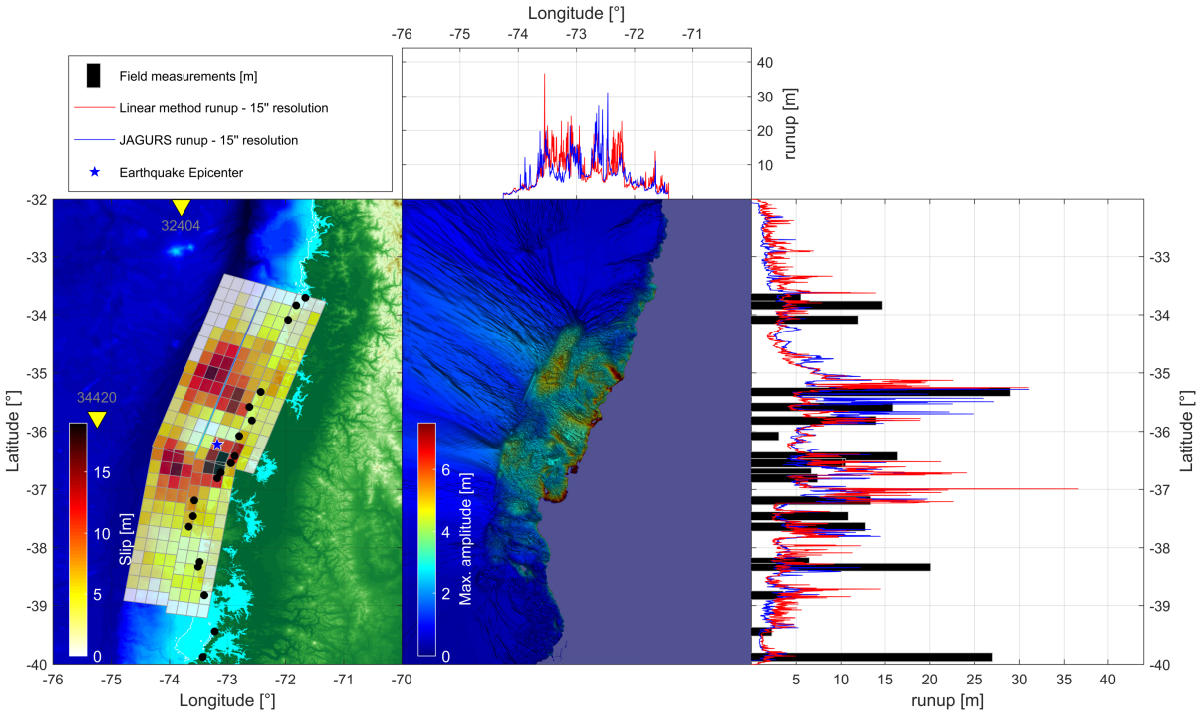

Fig. S16: Summary of the tsunami simulation for The 2010 Chile Earthquake with a finite fault model.

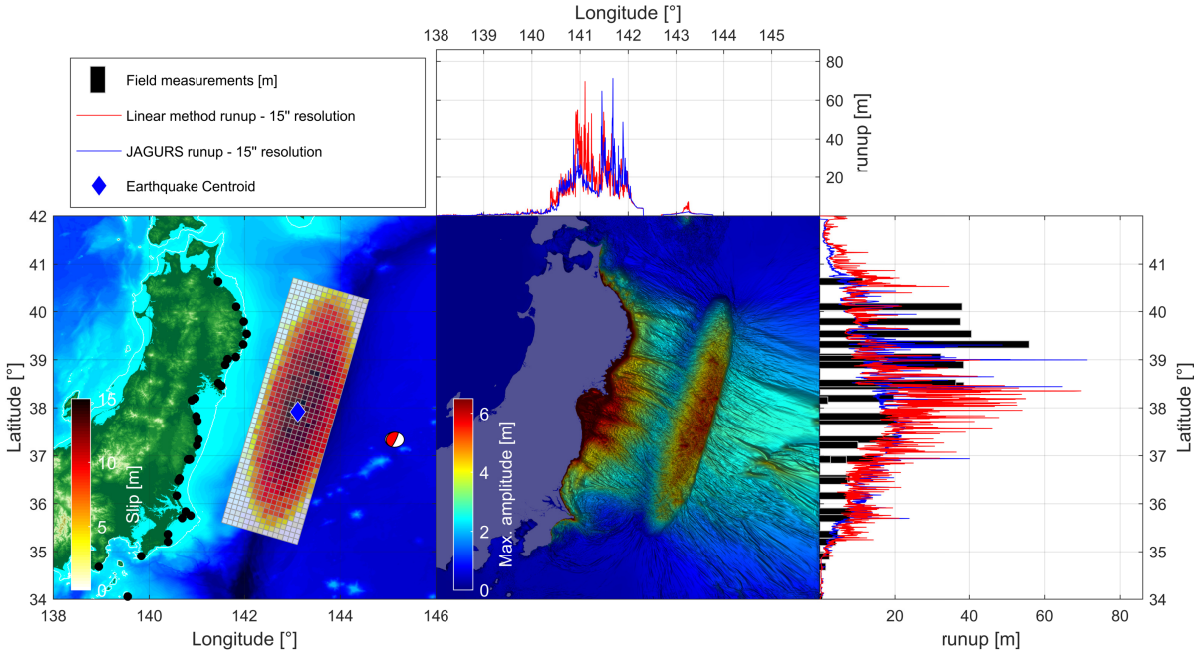

Fig. S17: Summary of the tsunami simulation for The 2011 Japan Earthquake with an elliptic source.

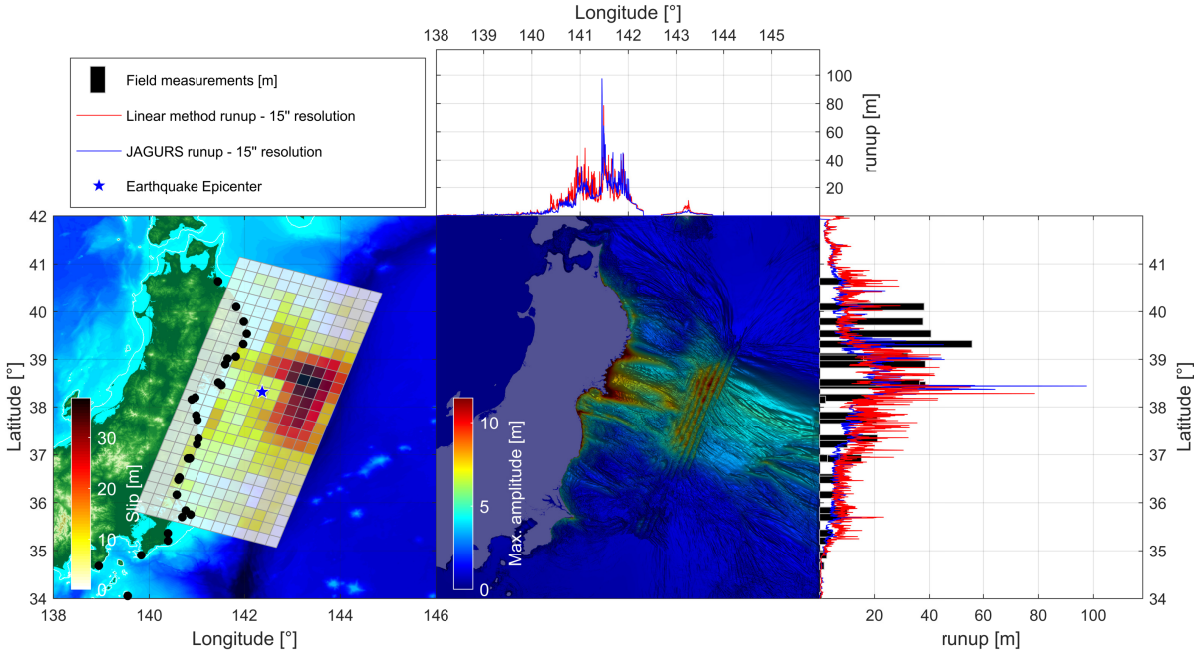

Fig. S18: Summary of the tsunami simulation for The 2011 Japan Earthquake with a finite fault model.

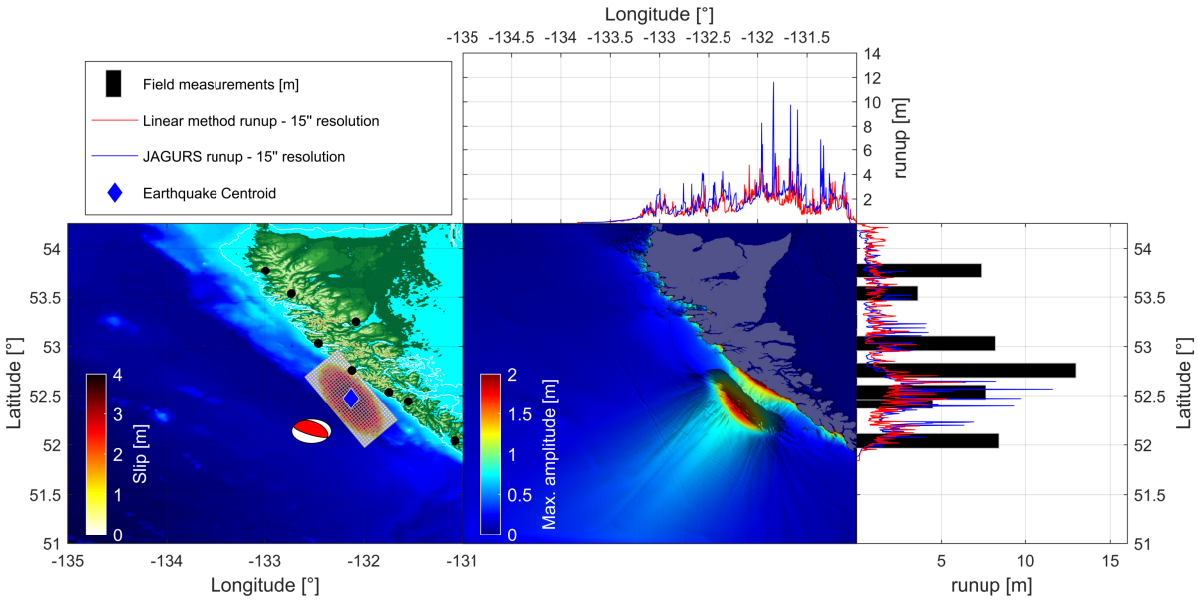

Fig. S19: Summary of the tsunami simulation for The 2012 Canada Earthquake with an elliptic source.

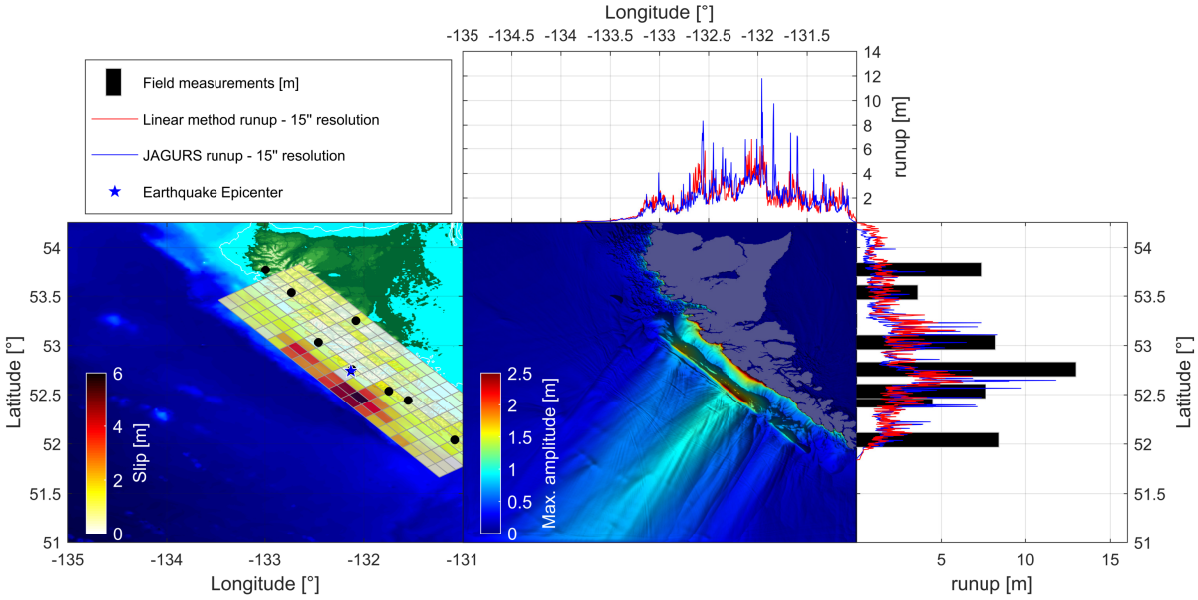

Fig. S20: Summary of the tsunami simulation for The 2012 Canada Earthquake with a finite fault model.

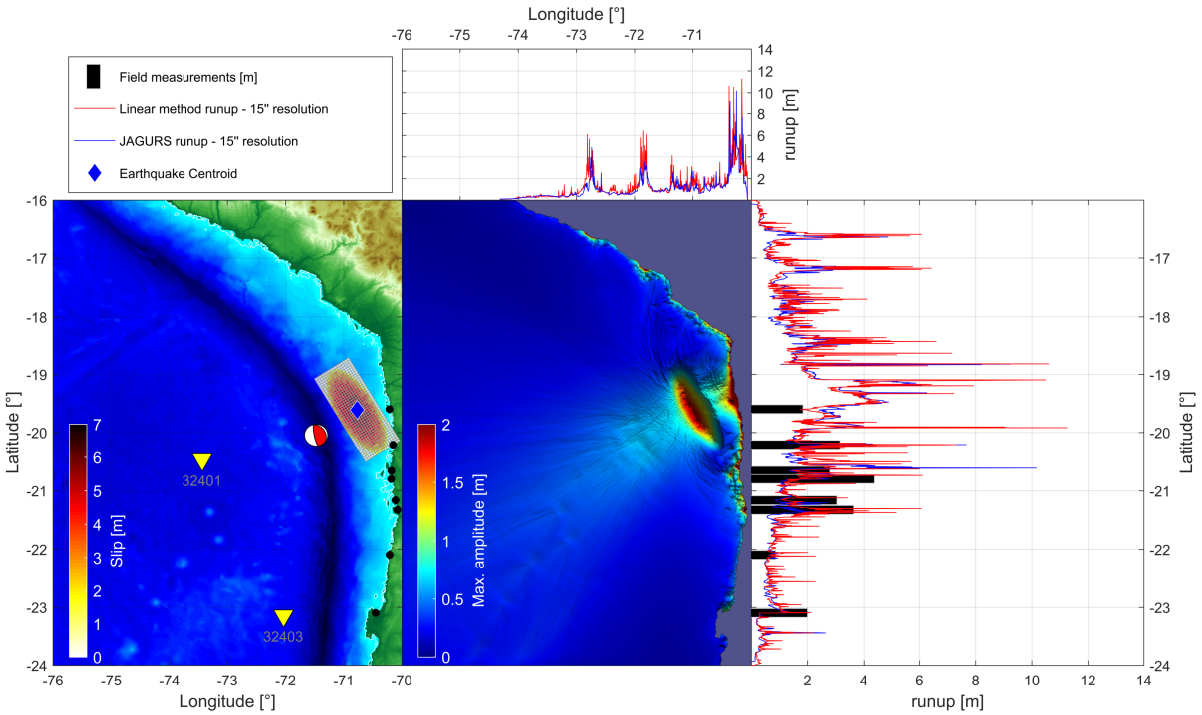

Fig. S21: Summary of the tsunami simulation for The 2014 Chile Earthquake with an elliptic source.

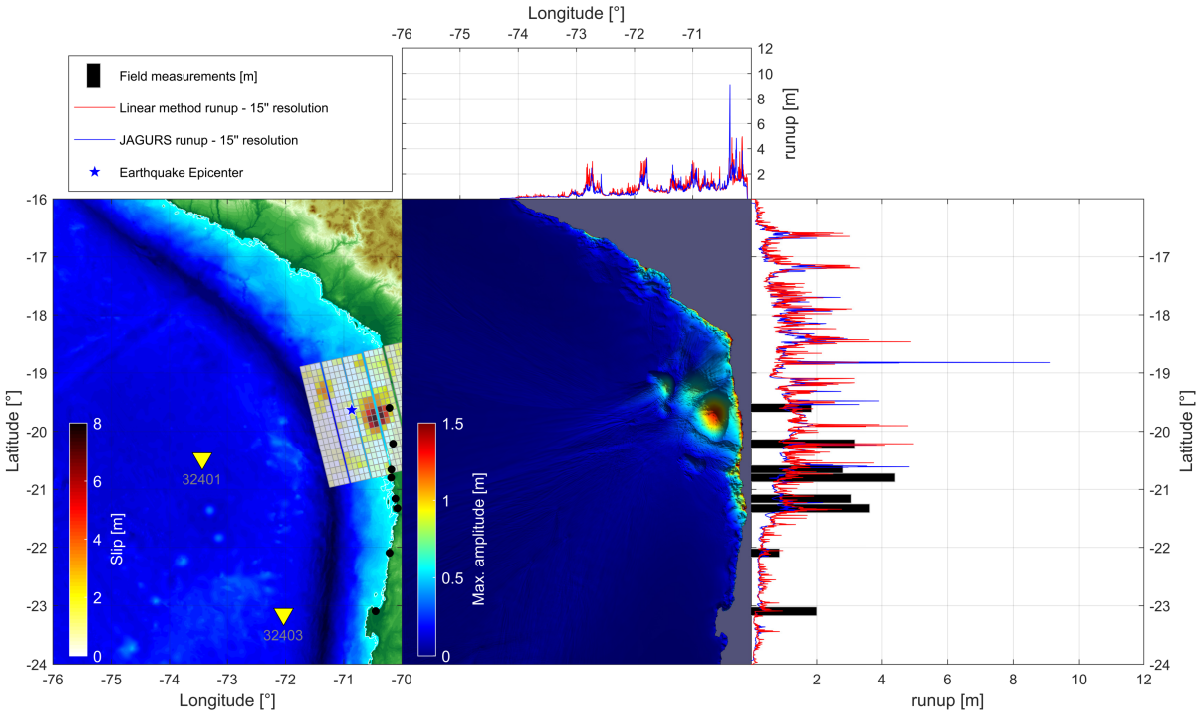

Fig. S22: Summary of the tsunami simulation for The 2014 Chile Earthquake with a finite fault model.

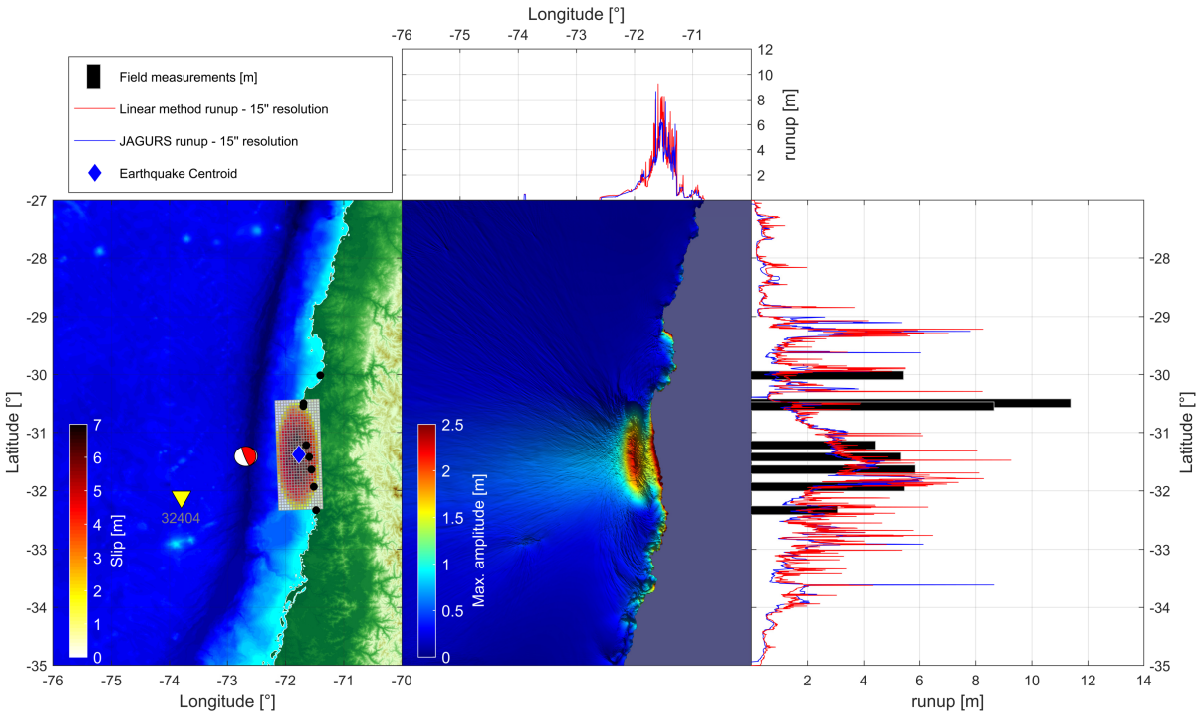

Fig. S23: Summary of the tsunami simulation for The 2015 Chile Earthquake with an elliptic source.

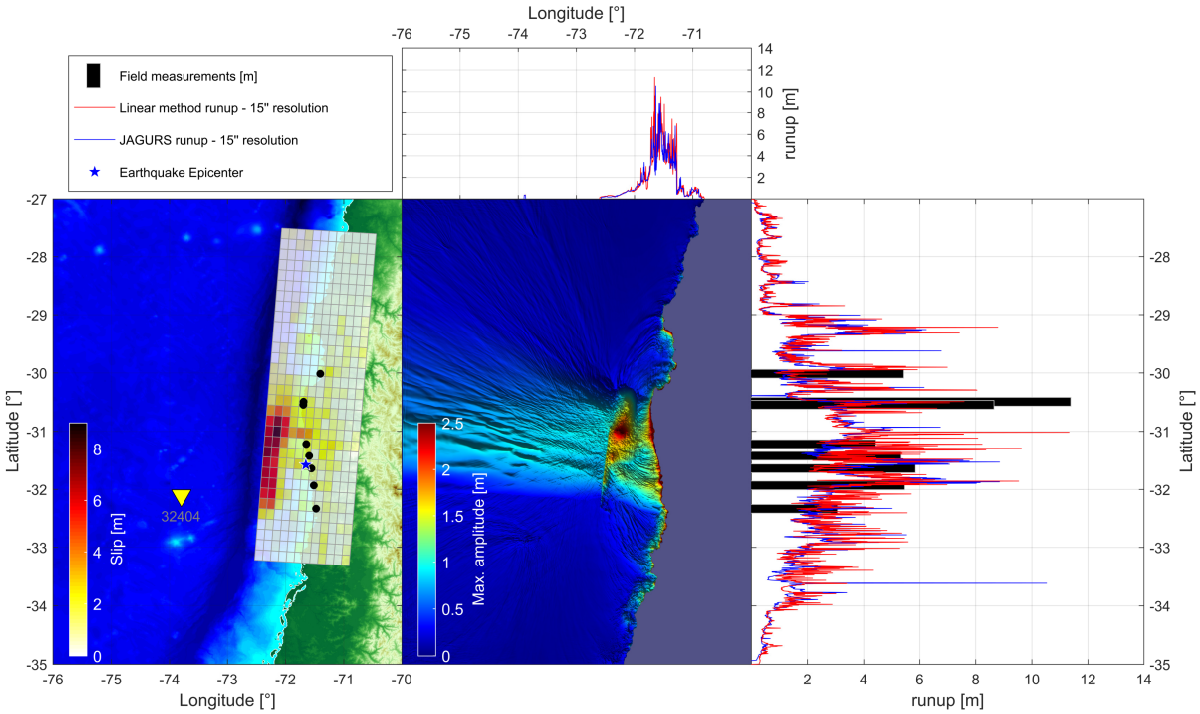

Fig. S24: Summary of the tsunami simulation for The 2015 Chile Earthquake with a finite fault model.